View metadata, citation and similar papers at core.ac.uk

brought to you by CORE

provided by University of Denver

University of Denver

Digital Commons @ DU

Electronic Theses and Dissertations

Graduate Studies

1-1-2012

Computationally Efficient Finite Element Models of the Lumbar Spine for the Evaluation of Spine Mechanics and Device Performance

Sean D. Smith
University of Denver

Follow this and additional works at: https://digitalcommons.du.edu/etd

 Part of the Computer-Aided Engineering and Design Commons

Recommended Citation

Smith, Sean D., "Computationally Efficient Finite Element Models of the Lumbar Spine for the Evaluation of Spine Mechanics and Device Performance" (2012). *Electronic Theses and Dissertations*. 612.
https://digitalcommons.du.edu/etd/612

This Thesis is brought to you for free and open access by the Graduate Studies at Digital Commons @ DU. It has been accepted for inclusion in Electronic Theses and Dissertations by an authorized administrator of Digital Commons @ DU. For more information, please contact jennifer.cox@du.edu,dig-commons@du.edu.

Computationally Efficient Finite Element Models of the Lumbar Spine for the Evaluation of Spine Mechanics and Device Performance

_____

A Thesis

Presented to

The Faculty of Engineering and Computer Science

University of Denver

_____

In Partial Fulfillment

of the Requirements for the Degree

Master of Science

_____

By

Sean D. Smith

March 2012

Advisor: Paul J. Rullkoetter

Author: Sean D. Smith
Title: COMPUTATIONALLY EFFICIENT FINITE ELEMENT MODELS OF THE LUMBAR SPINE FOR THE EVALUATION OF SPINE MECHANICS AND DEVICE PERFORMANCE
Advisor: Paul J. Rullkoetter
Degree Date: March 2012

ABSTRACT

Finite Element models of the lumbar spine are commonly used for the study of spine mechanics and device performance, but have limited usefulness in some applications such as clinical and design phase assessments due to long analysis times. In this study a computationally efficient L4-L5 FSU model and a L1-Sacrum multi-segment model were developed and validated. The FSU is a functional spine unit consisting of two adjacent vertebral bodies, in this case L4 and L5. The multi-segment model consists of all lumbar vertebrae and the sacrum. The models are able to accurately predict spine kinematics with significantly reduced analysis times, relative to fully deformable representations. Analysis times were reduced from 3 hrs and 20 min to 2 min and 1 min for the multi-segment and FSU models, respectively. The vertebrae geometries were reconstructed from CT scans of the cadaveric specimen. Prior to model development, experimental testing was performed on the specimen using a custom multi-axis spine simulator. Collection of kinematic data in response to external loading made tuning of the model stiffness possible. The improved computational efficiency of the models makes them more useful for applications requiring multiple iterations and short analysis times such as clinical and design phase assessments of implants. The model can also be used in efforts to develop lumbar musculoskeletal models, which may require multiple runs for the optimization of muscle forces.

TABLE OF CONTENTS

LIST OF FIGURES

LIST OF TABLES

CHAPTER 1 – INTRODUCTION

Low back pain affects many people and treatment of this affliction requires an understanding of spine mechanics. An effort to understand spine mechanics has been undertaken by both experimental and computational researchers. Spine simulators have been developed for pure moment loading of cadaveric spines to obtain range of motion information and servohydraulic test frames are used for axial compression testing. Experimental studies are the foundation of biomechanics research and provide a wealth of kinematic information in response to external loading. The use of numerical simulations to study orthopaedic biomechanics is made possible by experimental studies, which provide the data needed to validate the numerical models. Existing numerical models have been developed in both rigid body and finite element analysis platforms. Rigid body models are useful for prediction of spine kinematics, but are unable to predict internal stresses and strains. The explicit finite element platform is able to predict internal stresses and strains of vertebral bodies, soft tissues, and implants, as well as being able to handle complex loading conditions and contact. Finite element analysis is becoming an accepted practice for making biomechanical evaluations and orthopaedic implant testing. The cervical spine is commonly modeled using FE software in an attempt to understand dynamic whiplash injuries, but lumbar models are the most numerous due to the prevalence of low back pain. Existing lumbar FE models range from functional spine units (FSUs) consisting of two adjacent vertebrae, to full multi-segment

models that include vertebral bodies L1 through the sacrum. These models typically include the primary soft tissue structures, including the intervertebral disc and major ligaments. The inclusion of deformable soft tissues in the model is important for understanding the mechanisms of spine degradation, but when evaluating spine mechanics and device performance these deformable structures make analysis run times excessive. Therefore, although current numerical models that include deformable soft tissues are valuable for the evaluation of healthy spine mechanics and understanding spine degradation and the causes of low back pain, a computationally efficient lumbar model is needed for the timely evaluation of implant performance and the effects on spine kinematics.

The objective of this study was to develop a computationally efficient L4-L5 FSU model and L1-S1 multi-segment model. This was accomplished by representing the constraint provided by the soft tissue structures with mechanical joints between adjacent vertebrae. Previous efforts have used ball and socket joints between adjacent vertebrae to represent the rotational degrees of freedom and fully constrained the translational degrees of freedom. This method was effective in reproducing the torque-rotation behavior of the spine, however, spine motion is not purely rotational and thus this method is not a fully accurate representation of spine motion. All 6 rotational and translational degrees of freedom can be accounted for using bushing connecter elements between adjacent vertebrae. These connector elements provide appropriate torque-rotation and force-displacement constraint in the absence of the soft tissue structures.

When surgical intervention is used to treat low back pain it is common for certain ligament structures to be removed at the affected level. A model that can represent an

FSU with various soft tissue structures having been resected would be a powerful tool in assessing device performance and the effects of removing certain soft tissues. Such a model could also be used to study the contributions of individual structures to the overall stiffness of the segment. A secondary objective of this study was to develop a computationally efficient L4-L5 FSU with segmental stiffness properties of the bushing connector element tuned to represent the FSU with varying amounts of intact soft tissue structures.

Chapter 2 details background information on lumbar spine anatomy, injury mechanisms and treatments, quantifying spine kinematics in experiment, current spine models, the capabilities of explicit FE solvers, and optimization techniques. Chapters 3 and 4 describe the biomechanical testing of the L4-L5 FSU and L1-S1 segment, as well as the development and validation of the computationally efficient FSU and multi-segment models. Chapter 5 is a demonstration of a potential application of the models. The intact FSU model is implanted with a posterior stabilization device and predicts changes in range of motion. Results are compared to the fully deformable FSU model.

CHAPTER 2 – BACKGROUND

2.1 Anatomy of the Lumbar Spine

The vertebral column is comprised of twenty four vertebrae, connected by intervertebral discs (IVD) and ligaments. The lumbar spine consists of the lowest 5 vertebrae of the spinal column, adjacent on the top and bottom to the twelfth vertebrae of the thoracic spine region and the sacrum, respectively. The lumbar vertebrae are the largest segments of the vertebral column and are aligned in lordosis, a slight backwards curvature (figure 2.1). The vertebra is comprised of several components. The vertebral body is large and solid, and supports the weight of the cranium and trunk. It is composed primarily of cancellous bone, with a coating of cortical bone on the outer surface. The pedicles project backwards from either lateral side of the body. The laminae project backwards from the pedicles and meet in the posterior, completing the vertebral foramen which surrounds and protects the spinal cord. The spinous processes project backwards from the junction of the laminae, and serves as a muscle attachment site. The transverse processes project laterally from the pedicles and also serve as a muscle attachment site. The facet joints, or articulating processes, are located at the junction of the pedicles and the laminae. There are four facet joints on each vertebra, located on the inferior and superior processes to the left and right of the body, which articulate with adjacent vertebrae (figure 2.1). The intervertebral disc connects adjacent vertebrae and provides

some constraint to the segment. The intervertebral disc is composed of the nucleus pulposus in the center, surrounded by the annulus fibrosus (figure 2.1). The nucleus absorbs the impact of daily activities and the annulus distributes loads evenly across the disc. The vertebral segments are also stabilized by several ligament structures (figure 2.1). These ligaments are the anterior longitudinal (ALL), posterior longitudinal (PLL), ligamentum flavum (LFL), interspinous (ISL), supraspinous (SSL), intertransverse (ITL), and capsular ligament. The ALL and PLL connect the bodies, the ISL and SSL connect the spinous processes, the LFL connects the laminae, the ITL connects the transverse processes, and the capsular ligament connects the articulating facets (Gray 2001).

2.2 Low Back Pain

Low back pain (LBP) is a problem experienced by a majority of the population (Cerciello *et al., 2011)*. Some studies report that 80% of individuals will experience low back pain at some point in their lifetime. It limits peoples' ability to be physically active, causes suffering, and lowers quality of life. Other than the common cold, LBP more than any other ailment causes people to seek medical attention and take time off from work (Duquesnoy *et al*., 1998, Ekman *et al*., 2005, Krismur *et al*., 2007, Waddell *et al*., 2005, van Tulder *et al*., 2006). This is an expensive ailment due to both medical expenses and missed time from work (Krismer *et al*., 2007, Manek *et al*., 2005, Katz *et al*., 2006). Pain in the lower back occurs as a result of instability and degenerative changes. Disc degeneration, facet osteoarthritis, muscle alterations, and ligament degeneration can lead to instability, as well as other painful conditions. Instability results in greater than normal

mobility which can lead to abnormal loading of structures such as the facets and disc, and nerve impingement (Panjabi *et al*., 2003, Panjabi *et al*., 1992, Fujiwara *et al*., 2000, Gertzbein *et al.*, 1985, Dickey *et al*., 2002). There are several structural changes of the degenerated segment's disc and surrounding structures that can be used to characterize disc degeneration such as reduced intradiscal (ID) pressure, loss of disc height, reduced water content, tissue fibrotisation, proteoglycan loss, sclerosis of vertebral endplates, formation of fissures and osteophytes, annulus lesion, and herniation of the nucleus pulposus (figure 2.2). The primary source of pain as a result of disc degeneration is in the facet joints, bony endplates, and surrounding nerves. Loss of ID pressure and IVD height can result in the facets and endplates experiencing higher than normal loads. If the annulus tears and the nucleus pulposus bulges through the annulus wall, this can result in pressure being put on surrounding nerves (Vernon-Roberts *et al*., 1977, Noailly *et al*., 2011). Cadaver studies have demonstrated a direct correlation between the subject having a history of low back pain and tears in the annulus (Viderman *et al*., 2004). The mechanical progression of disc degeneration is unclear, but it is believed that abnormal loads and motion patterns may accelerate the process (Adams *et al*., 2005, Mulholland *et al*., 2008, Nakamura *et al*., 2009, Setton *et al*., 2006). Recent studies have shown that the presence of certain gene forms is associated with degenerative disc disease, suggesting that the disease is hereditary (Waddell *et al*., 2005, Jim *et al*., 2005).

2.3 Treatment of Low Back Pain via Surgical Intervention

2.3.1 Overview

Abnormal physiological loading of anatomical structures such as the facet joints and the IVD is a painful condition and the prevalence of this issue has resulted in the development of numerous medical devices and procedures to relieve these structures. As shown in figure 2.3, the most common procedures are fusion, total disc replacement (TDR), and dynamic stabilization , which is becoming more common (Don *et al*., 2008, Freeman *et al*., 2006, Galbusera *et al*., 2011, Sengupta 2004). Depending on the device and procedure, the disc may be fully or partially removed to alleviate pressure on adjacent nerves and relieve sciatic pain (Mixter et al., 1934), or to make room for a device. The disc is completely removed during total disc replacement procedures and is fully or partially removed during fusion procedures. In cases where degeneration and instability are less severe, the disc might be left intact in combination with an implanted dynamic stabilization device with the goal of adding stability while maintaining some range of motion, and unloading the disc and facets to reduce pain (Sengupta 2004). Patients should try conservative noninvasive treatments such as physical therapy and exercise before considering surgery (van Tulder *et al*., 2006). However, if noninvasive treatments are ineffective the various implants and procedures mentioned above have proven to be clinically effective at relieving low back pain (Ekman *et al*., 2007, Fritzell *et al*., 2003, Guyer *et al*., 2009, Zigler *et al*., 2007). Although these treatments are often

successful, there are various complications that tend to occur, which are described in the following sections.

2.3.2 Total Disc Replacement

Over the last ten years the frequency of TDR to treat low back pain has increased significantly (Freeman *et al*., 2006). When a total disc replacement procedure is performed the entire IVD is removed and replaced with an artificial articulating disc with an anterior approach. The goal of implanting the device is to reduce or eliminate pain and restore the functional mechanics of the disc, returning the segment to normal intervertebral space and mobility (Noailly *et al*., 2011). Ball on socket (BOS) designs are currently the best available devices for achieving close to normal segmental range of motion (figure 2.3, 2.4). The most commonly used of these devices that are available on the market are the CHARITE and the ProDisc. Both of these designs consist of a polyethylene core that articulates with two metallic endplates which are placed between and fixed to adjacent vertebrae. Both are considered to be clinically successful (Guyer *et al*., 2009, Zigler *et al*., 2007). Current BOS devices always consist of metallic endplates; however the articulating surface varies between metal and polyethylene (Berg 2011). Several studies, both long and short term, have reported that the clinical outcome of TDR is as good as or better than fusion (Lemaire *et al*., 2005, Tropiano *et al*., 2005, Bertagnoli *et al*., 2002, Bertagnoli *et al*., 2005, Chung *et al*., 2006, Le Huec *et al*., 2005, Lemaire *et al*., 1997, Shim *et al*., 2007, Siepe *et al*., 2006, Tropiano *et al*., 2003, Zeegers *et al*., 1999). Random controlled trials of the SB CHARITE and ProDisc for FDA approval both

claimed that TDR performed better than fusion (Blumenthal *et al*., 2005, Zigler *et al*., 2007). Because these devices allow for close to physiological mobility, the frequency of patients with ASD should decrease with respect to fusion devices (Dmitriev *et al*., 2008, Kanayama *et al*., 2009). Unfortunately there are limitations on who is potential candidate for TDR. If the degenerated segment has experienced spondylosis or has had facet joints removed then that patient typically cannot be a candidate (Anderson & Rouleau 2004, Blumenthal *et al*., 2005, Zigler *et al*., 2007). Although these designs are considered the best on the market at this point in time, there are still several challenges that they present. BOS implants have high axial stiffness. A healthy intervertebral disc acts as the shock absorber of the spine and allows for some axial compression. The high axial stiffness of BOS devices may lead to excessive compressive loading in adjacent segments. Additionally, the articulating endplates are allowed to slide freely over the polyethylene core, which can cause adjacent bony endplate damage and over flexibility at the treated segment (Sinigaglia *et al*., 2009). Overall, complications following ball and socket disc replacement procedures have been reported 80% of the time. The potential complications associated with total disc replacement are vertebral body fracture, prosthesis migration, spontaneous ankylosis, and accelerated facet degeneration. The most common complication following disc replacement is facet joint pain. The device's effect on the segment's motion, such as over flexibility, can lead to increased or abnormal loading of the facets. Placement of the device is an important factor in future complications due to the lack of various sizes and patient specificity with the devices (Freeman *et al*., 2006, Putzier *et al*., 2006, Siepe *et al*., 2008).

2.3.3 Fusion and Stabilization Devices

TDR is a method that aims to maintain normal segment mobility, but sometimes it is determined that instability in the degenerated segment is resulting in excessive mobility and positions that are painful (nerve impingement, abnormal facet loading) (Dickey *et al*., 2002, Fujiwara *et al*., 2000, Gertzbein *et al*., 1985, Harmon 1964, Mulholland 2008). When this is the case, stability is added to the segment using fusion or dynamic stabilization devices (figure 2.3, 2.4). Fusion is the most common and accepted practice to surgically treat low back pain (Galbusera *et al*., 2011, Don and Carragee 2008, Yan *et al*., 2011). Depending on a patient's level of instability, there are both fusion and non-fusion dynamic pedicle devices that are designed to limit the treated segment's range of motion and add stability. Fusion pedicle devices utilize a high stiffness rod, typically made from stainless steel or titanium, and are intended to prevent almost all motion at the treated segment due to high instability (Galbusera *et al*., 2011). There are several variations of the fusion procedure but all are designed to reduce pain in patients with DDS (Berg 2011). In general, when fusion of adjacent vertebrae is performed, two rods are placed in the posterior (posterior stabilization devices) and fixed to the vertebral bodies with pedicle screws penetrating the pedicles and in to the vertebral bodies. The disc is commonly fully or partially removed in order to place a spacer device between the vertebrae to maintain the intervertebral disc space. Additionally, bone grafts or bone substitutes may be placed between the spinous process and along the rods to help achieve total fusion at the treated level. The procedure uses a posterior approach (Berg 2011). The specific devices and materials may vary, as well as the device placement, but ultimately

the clinical outcomes are the same (Ekman *et al*., 2007, Fritzell *et al*., 2003). Fusion was shown to provide total pain relief in 29% of patients and an improvement with the amount of pain in 63% of patients (Fritzell et al., 2001).

To treat a segment experiencing minor instability, a dynamic stabilization device may be used. Like solid fusion rods, dynamic rods are also commonly made from stainless steel or titanium but incorporate a flexible component, in some cases made from polycarbonate-urethane, to add some flexibility to the rod (Galbusera *et al*., 2011). Also similar to the fusion rods, the dynamic rods are fixed to the vertebral bodies in the posterior through the pedicles. These devices are designed to maintain some of the mobility of the segment, but avoid extreme motions that are potentially painful. Dynamic stabilization devices unload the disc and facets, which may also relieve pain (Sengupta 2004, Wilke *et al*., 2009). The IVD is typically left intact during dynamic stabilization procedures.

Adjacent segment degeneration or adjacent segment disease (ASD) is a common complication following lumbar fusion. The mechanism that causes ASD is not well understood, but lumbar fusion, which restricts range of motion and unloads anatomical structures at the treated level, can lead to a concentration of mechanical stress on adjacent discs and articular facets (Yan *et al*., 2011). Conditions that are considered forms of ASD are accelerated disc degeneration, herniation of nucleus pulposus, acquired spondylolysis, segment instability, spinal stenosis, and arthritis of the posterior facet joints (Min *et al*., 2008). Degenerative changes can be detected in adjacent segments using radiography as early as 25 months after fusion (Aota *et al*., 1995). A study that tried to understand the mechanism of ASD found that when adjacent discs were already degenerated, stress

changes were found in these adjacent discs, but when adjacent discs were healthy, fusion did not induce stress changes. They concluded that the single level of posterior fusion in the lumbar spine accelerates degeneration of adjacent segments if degeneration already exists (Yan *et al*., 2011). They found that risk factors related to ASD were age, length of fusion, use of internal fixation, and condition of adjacent segment (Yan *et al*., 2011).

2.4 Description of Spine Motion

The lumbar spine leans slightly backwards in an alignment called lordosis. The lumbar region of the spine has a large range of motion, second only to the cervical region. On average, the range of motion of a lumbar FSU is 10 degrees flexion, 5 degrees extension, 5 degrees lateral bending, and 3 degrees axial rotation. Translations are small relative to rotational degrees of freedom, but nonzero. It is difficult to obtain in vivo kinematics of the spine (Cerciello *et al*., 2010). It is possible to roughly obtain this data using radiography where images are typically captured only at end of range of motion positions to limit the subject's exposure to radiation. The path of the vertebral bodies from start to end position is estimated (Cerciello *et al*., 2010). A more complete path of the spine motion can be captured using fluoroscopy due to the lower x-ray dosage associated with these devices. Single plane fluoroscopy provides useful information for in plane motions such as flexion and extension but does not provide information on out of plane rotations. Bi-planar fluoroscopy has the capability to capture 3D motions, but these devices are not widely available (Anderst *et al*., 2007). Characterizing healthy spine

kinematics would provide baseline data for comparison which could be used to identify degeneration and instability in a spine segment.

2.5 Experimental Spine Simulators

Many studies have examined the biomechanical response of the lumbar spine subject to external loading. These studies typically use simplified loading conditions such as pure moments and compressive forces to simulate basic movements such as flexion-extension, lateral bending, axial rotation, and axial compression (Rohlman *et al*., 2009a, 2009b). Experimental spine simulators have been developed by research groups to more accurately simulate pure moment loading and hydraulic test frames such as Instron (Instron, Norwood, MA) and MTS (MTS, Eden Prairie, MN) systems have been used to simulate compressive loading to characterize the mechanics of the spinal column in response to various external loads.

Experimental testing of cadaveric lumbar spine specimens was performed at University of Washington's Applied Biomechanics Lab (UW, Seattle, WA) using their multi-axis spine simulator (figure 2.5). This simulator has computer controlled multi-axis loading, adjustable follower load, kinematic data collection using Vicon motion capture (Vicon Motion Systems, Los Angeles, CA), and intradiscal pressure measurement. The simulator can apply pure bending about a single axis or combined loading about multiple axes at both quasi-static and dynamic rates. Pure moments are applied to the cephalad end and the caudal end is fixed to a 6-axis load cell to collect force and moment data that is transmitted through the spine.

2.6 Previous Numerical Spine Models

2.6.1 Rigid Body Models

There have been many spine models developed within rigid body modeling platforms, most commonly within the open source platform OpenSim (Stanford University) and the relatively new commercial software AnyBody (AnyBody Technology, Denmark). These platforms are especially useful for musculoskeletal modeling because they are computationally inexpensive and can provide useful information about muscle activation and segment kinematics. A recent study at UCSF developed a lumbar model in OpenSim which they consider to be the "the most physiologically detailed non-commercial musculoskeletal model available" (Christophy *et al*., 2011). The model incorporated detailed musculature with patient specific bone geometries. The motions of flexion, extension, lateral bending, and axial rotation were simulated and driven by varying muscle activation patterns. Many lumbar models have been developed in open-source and commercial platforms and have been documented in the literature (Lambrecht *et al*., 2009, Liu *et al*., 2011, Huynh *et al*., 2010, El-Rich *et al*., 2004, de Zee *et al*., 2007). These rigid body platforms can be useful in understanding the pathology behind low back pain through the comparison of healthy and degenerated spine kinematics, but lack the ability to predict information about contact in the facets, strains in the annulus fibrosus, intradiscal pressure, bone strains, and strains in an implanted device.

2.6.2 Finite Element Models

As noted by Yan *et al*., 2011, finite element (FE) analysis has been used successfully in the field of biomechanics. Researchers have begun to use finite element models to assess the biomechanics of the lumbar spine and to understand spine degeneration. FE models rely on kinematic and kinetic data from experimental studies for model development and validation. FE models are capable of predicting mechanical parameters of interest that cannot be measured through experimentation, such as internal stresses and strains of deformable structures (Ugur *et al*., 2011, Yan *et al*., 2011). FE models eventually could reduce our dependence on cadaveric testing and experimentation on animals (Yan *et al*., 2011). Modeling of the spine using FE platforms is becoming a complement to biomechanical experimentation and is recognized for its usefulness in assessing medical device performance (Ugur *et al*., 2011, Yan *et al*., 2011, Lu *et al*., 1996, Zander *et al*., 2001, Natarajan *et al*., 2005, Shirazi *et al*., 1984, Schmidt *et al*., 2010, Jones *et al*., 2008). The spine geometries are commonly reconstructed from computed tomography scans (Goel *et al*., 1995, Liebschner *et al*., 2003). This creates an accurate geometry and avoids over-simplification with the use of generic shapes. Many commercial and homegrown mesh generation softwares are available. Material properties of the spinal tissues have been documented in the literature following extensive testing (Ugur *et al*., 2011). Parameters that are commonly used to validate a model are ROM, IDP, bone strain, ligament deformation, and facet force prediction. Experimental testing data on these parameters is becoming more available in the literature (Adams *et al*., 1996, Frei *et al*., 2001, Herver *et al*., 2007, Sawa *et al*., 2008, Wilson *et al*., 2006). Validating

the models ability to accurately predict range of motion is important for the model to be used to assess device performance (Ugur *et al*., 2011). An advantage of the explicit FE platform is that it allows for structures to be modeled as rigid or deformable. It is common to represent bones as rigid due to their high stiffness relative to soft tissues, which saves computational time (Ugur *et al*., 2011).

2.7 The Explicit Finite Element Platform

Implicit FE analysis has been and continues to be more common for solving biomechanics problems. A major issue with using the implicit solver to model quasi-static and dynamic processes such as joint motion is the assumption that structures in the model are statically loaded. Motions of the spine in vivo are controlled by muscle forces and constrained by surrounding soft tissues (Godest *et al*., 2002). Explicit analyses have become more commonly used for the study of the performance of total knee replacement devices and the cervical spine due to the dynamic nature of the motion and loading that these structures experience. Convergence has been an issue for implicit solvers when trying to simulate dynamic activities. Implicit FE analysis is also computationally expensive, especially when solving contact problems. Explicit FE code can be used to predict spine kinematics and internal stresses and strains simultaneously in a single analysis. It also produces a stable solution and at lower computational cost relative to implicit solvers. The use of Explicit FE analysis is advantageous when simulating complex motions and loading consistent with those used in experiment (Godest *et al*., 2002). Dynamic analyses take into account inertia effects. Density must be defined for all

materials and each degree of freedom must have mass and rotary inertia associated with it. The increments are relatively inexpensive compared to the increments in the implicit integration method. In implicit analyses the integration operator matrix must be inverted and a set of nonlinear equilibrium equations must be solved at each time increment. For the explicit scheme analysis times only rise linearly with problem size, whereas run times for implicit integration increase much more rapidly. Explicit dynamic analyses present several advantages over implicit analyses. These analyses are computationally efficient for the analysis of large models with relatively short dynamic response times and the analysis of extremely discontinuous events or processes. Additionally, the inclusion of general contact conditions is allowed, and models can undergo large rotations and deformations. The procedure performs a large number of small time increments efficiently. It uses an explicit central-difference time integration rule, which is relatively inexpensive compared to the direct integration used in standard analyses because there is no solution for a set of simultaneous equations. The computational efficiency also comes from the use of diagonal element mass matrices and small time increments, which allow the solution to proceed without iterations and without requiring tangent stiffness matrices to be formed. The time increment is based on the smallest element edge length in the model. It also simplifies the treatment of contact. The advantages associated with the explicit platform can be applied to quasi-static processes (Abaqus 2010).

2.8 Optimization Techniques

Optimization is commonly used in engineering applications to select the best design when multiple designs are available. It is a process of guessing and searching for the minimum or maximum of a function (Chapra 2010). The function to be optimized is referred to as the objective function. A commonly used global optimization algorithm is adaptive simulated annealing (ASA). ASA is a more efficient version of the simulated annealing (SA) technique. The SA techniques are used to find the global optimum of a function. The name is derived from the physical process of heating up and slowly cooling materials so that the crystalline structures settle in to a state of lower potential energy (Venkatarman 2009). ASA works well with nonlinear problems with short running simulations and can effectively distinguish between different local optima (Isight 2010).

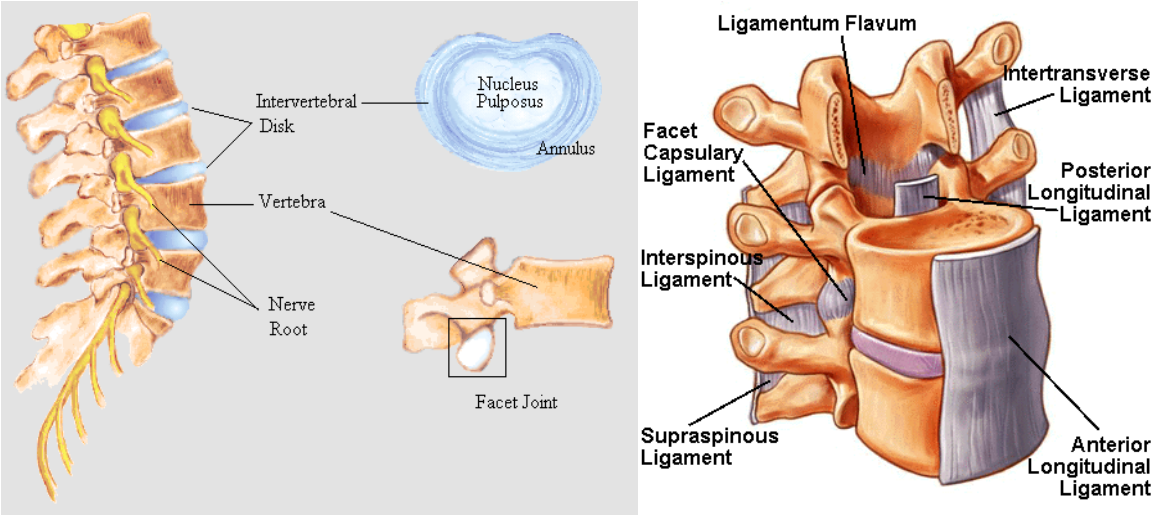

Figure 2.1 L1-S1 lumbar segment of the human spine (left) and osteoligamentous structures of the lumbar spine (right) (www.spineuniverse.com, 2011).

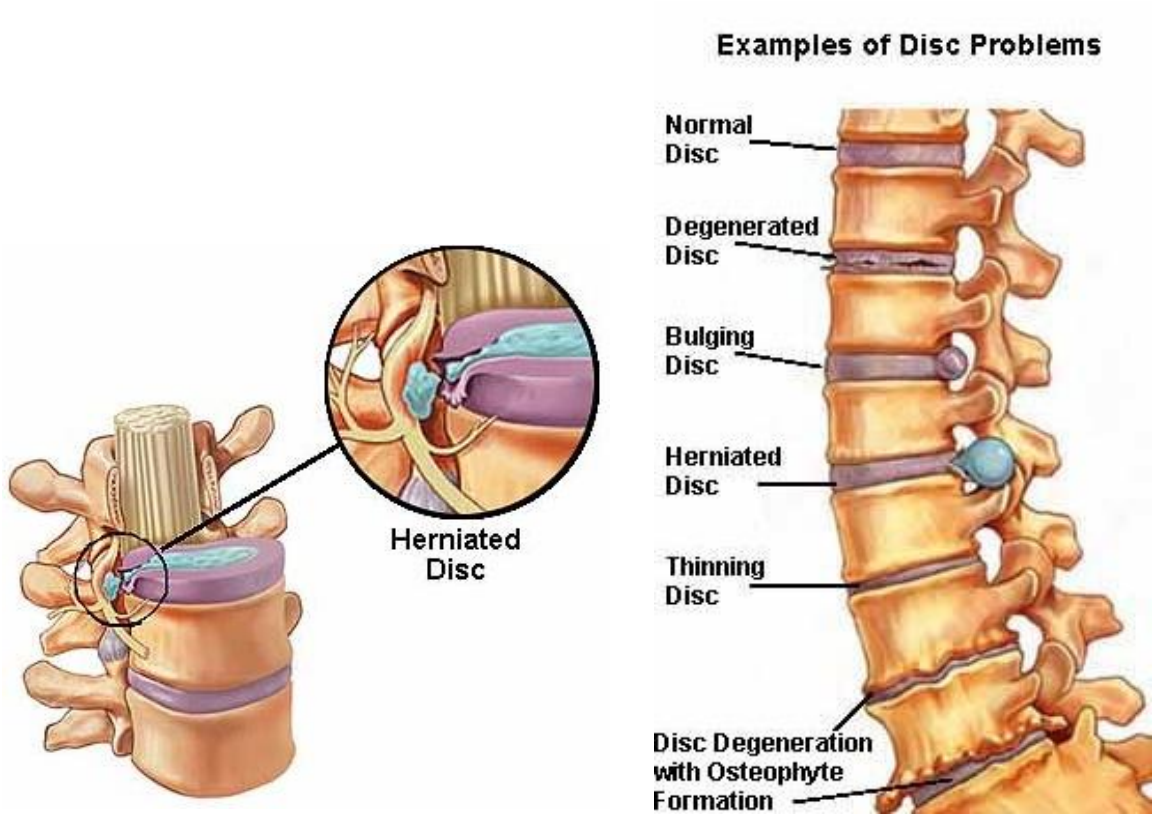

Figure 2.2 Illustration of herniated disc applying pressure to surrounding nerve root (left) and the various forms of disc degeneration (right) (www.spineuniverse.com, 2011).

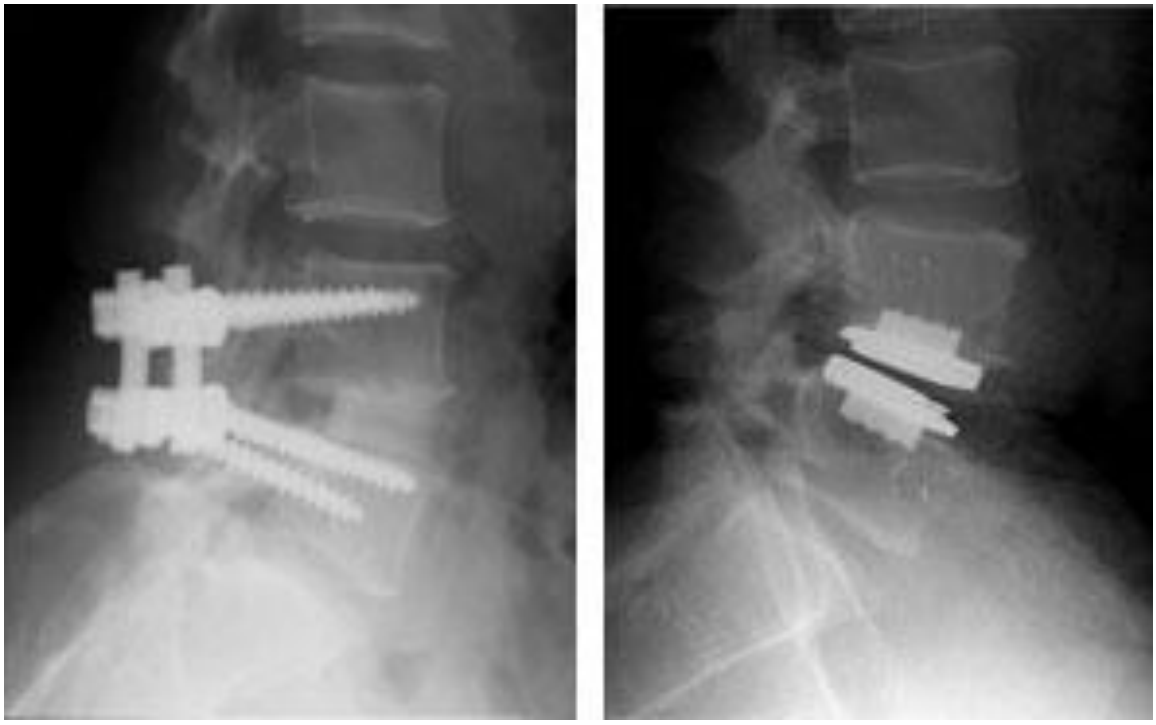

Figure 2.3 Computed tomography images showing implanted lumbar fusion rods (left) and ball on socket total disc replacement device (right) at the L4-L5 level (us.synthesprodisc.com).

Figure 2.4 Ball on socket total disc replacement device with metallic endplates and polyethylene core (left) and dynamic posterior stabilization device with pedicle screws (right) (Murtagh *et al*., 2011, us.synthesprodisc.com, 2011).

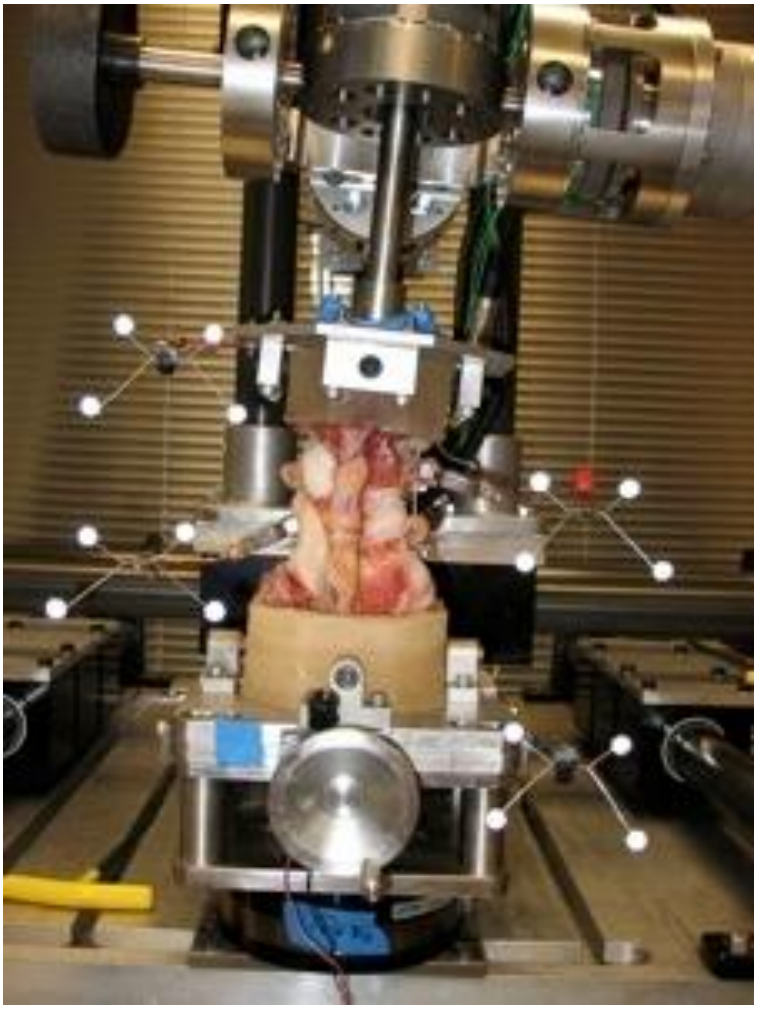

Figure 2.5 University of Washington Applied Biomechanics Lab Multi-Axis Spine Simulator.

CHAPTER 3 – TUNING OF FINITE ELEMENT MODEL – PREDICTED FSU KINEMATICS WITH SEQUENTIAL SECTIONING PROTOCOL

3.1 Introduction

The mechanics of the lumbar spine are often studied by isolating a single motion segment. In cadaveric experiments, it is common that the full lumbar segment will undergo testing and then be reduced down to functional spine units (FSUs) for more detailed testing at that specific level. The FSU has some limitations. The prevalence of adjacent segment degeneration (ASD) following instrumentation of a degenerated segment has made the mechanics of the adjacent segments a point of high interest. Despite this limitation, FSUs are still useful for understanding spine mechanics at a specific level and evaluating medical device performance.

FSU FE models are also quite common. A validated FSU model can be used to evaluate changes in ROM and loading in the disc and facets following device inclusion. The model can also predict strains in the bones and device. This can be useful for prediction of the devices performance at the treated level. Run times for FSU models are also significantly less than full segment models which make them more practical for clinical and design phase assessments.

3.2 Methods

3.2.1 Experimental Kinematic Analysis

Prior to developing the FE L4-L5 model, experimental testing of the FSU was completed at the University of Washington's Applied Biomechanics Lab to support the development and validation of lumbar spine FEA models at the University of Denver Computational Biomechanics Lab. Four fresh and frozen human lumbar spines were tested, two of which were reduced down to L2-L3 and L4-L5 FSUs. Prior to testing, the spines were inspected visually and using x-ray screening to evaluate the condition of the spines. One specimen was selected with no to mild degeneration, two specimens were selected with mild to moderate degeneration, and one was selected with moderate to severe degeneration for biomechanical testing. Four radio-opaque marker beads that were 4mm in diameter were embedded into each vertebral body for measurement of the segment kinematics. The beads were burrowed in to the bone and fixed with cyanoacrylate glue. High resolution computed tomography (CT) scans were obtained for each specimen with a GE LightSpeed CT scanner with 0.6mm slice thickness so that geometries could later be reconstructed and the vertebral kinematics could be applied to the reconstructed markers. Prior to testing all surrounding soft tissues were removed other than the osteoligamentous structures and the intervertebral disc. Screws were placed in the ends of L4 and L5 and the vertebral bodies were potted in poly-methylmethacrylate. The FSUs were tested using a sequential sectioning protocol to assess the contribution of the transected structures to the mechanical stability of the segment. Pure moment testing of the FSU was performed using the Applied

Biomechanics Lab's custom multi-axis spine motion simulator and spine segment motions were recorded using a 4 camera motion capture system. Pure moments were applied using 3 independently operated rotary actuators on air bearings to allow translations in x,y, and z. The FSUs were first evaluated with all soft tissues intact, and then testing was performed following the removal of each soft tissue structure until only the disc remained, subject to pure moment loading (flexion, extension, lateral bending, and axial rotation). Following testing of the intact FSU, structures were removed in the order of the supraspinous ligament, interspinous ligament, posterior longitudinal ligament, anterior longitudinal ligament, intertransverse ligament, facet capsules, and lastly the facets. Pure moments were applied to the cephalad end and the caudal end was fixed to a 6-axis load cell to collect force and moment data that is transmitted through the spine. Pure moments of 10Nm were applied while testing the intact FSU, and then a hybrid loading procedure was followed for the sectioning protocol. For hybrid loading, a pure moment was applied until the maximum angle recorded during the intact testing was reached. The FSUs were also tested in axial compression after the last sectioning step using a MTS servohydraulic test frame to find the axial compression stiffness of the intervertebral disc. The compression testing was displacement controlled and the FSU was compressed until a load in the range of 1,000 – 1,500 N was delivered.

3.2.2 Finite Element Model of L4-L5 FSU

A specimen specific L4-L5 FSU FE model was developed in Abaqus/Explicit (Simulia, Providence, RI) from high-resolution computed tomography scans of an adult

cadaveric spine. The spine was that of a 71 year old male who was 68" tall and weighed 267 lbs. The spine was considered to be mild to moderately degenerated with a disc grade of 3-4. The scans were imported into ScanIP (Simpleware, Exeter, UK) as dicom files and the spinal geometry was reconstructed manually by selecting the bone portion of each image. The reconstructed geometry consisted of vertebral bodies L4 and L5. These geometries were brought in to Hypermesh (Altair, Troy, MI) for mesh generation. The vertebrae were represented as rigid bodies and were meshed with 3 node triangular shell elements. All soft tissue structures such as the ligaments, intervertebral disc, and facet cartilage were excluded from the model. The inclusion of deformable soft tissue structures in the model contributes significantly to analysis time. A 6 degree of freedom bushing connector element was placed between L4 and L5 at a point equidistant from the superior and inferior end plates and centered in the medial-lateral and anterior-posterior directions. The stiffness of this connector element was responsible for providing the appropriate torque-rotation and force-displacement constraint in the absence of the soft tissue structures. Nonlinear stiffness curves were defined for each degree of freedom of the connector element and properties were optimized to reproduce the kinematic-moment measured response from experiment. The bushing connector consists of two coincident nodes placed between vertebrae. One of the nodes is fixed and beamed to the L5 rigid body reference node, while the other node is beamed to the L4 rigid body reference node and is free to rotate and translate. The use of the bushing connector element to represent soft tissue constraints is an improvement upon the use of a ball and socket joint between vertebrae. The ball and socket representation can accurately provide the appropriate restraint for the rotational degrees of freedom, but fully constrains translational degrees

of freedom. Although translations of vertebral bodies are small relative to the rotations they experience, they are not negligible and must be accounted for in order to have a true representation of spine motion. A dummy element was defined with bone properties whose edge length was used for calculation of time increment size within the explicit solver.

3.2.3 Computational Kinematic Analysis

Tuning of the L4-L5 FSU was based on torque-rotation and force-displacement data obtained from the biomechanical testing of this cadaver specimen at the University of Washington's Applied Biomechanics Lab. Fiducial marker positions were extracted from the CT scans at the time the bone geometries were reconstructed. The kinematic data collected on the vertebral segment motion with the Vicon motion capture system during experimental testing was used to drive the motion of the segment in flexion, extension, lateral bending, and axial rotation. L5 was constrained in all degrees of freedom and the motion of L4 was driven using the recorded marker positions. For tuning of rotational degrees of freedom, reaction moments at the fixed node of the bushing connector element and rotations at the L4 rigid body reference node were requested as outputs from the simulation and plotted against the torque-rotation response measured in the experiment. For tuning of translational degrees of freedom, the above procedure was repeated with reaction forces and translations being requested as the outputs. Optimization of the bushing properties was performed in Isight (Simulia, Providence, RI) using adaptive simulated annealing. The objective function that was minimized was the

sum y-squared difference between the model predicted and experimentally measured torque-rotation and force-displacement response of the FSU in flexion, extension, lateral bending, and axial rotation, while the stiffness parameters were allowed to vary. This procedure was performed for the intact FSU and for each of the sequential sectioning steps until only the disc remained. The disc only FSU was tested in compression. A concentrated load of 1000 N was applied to L4 and the displacement of L4 was requested as an output. The force-displacement response of the model was plotted against the experimental response and the axial stiffness parameters were optimized to reduce the error between the two curves.

3.3 RESULTS

Torque-rotation and force-displacement behavior for the optimized FSU model represented the experiment well in flexion, extension, lateral bending, axial rotation, and compression. Analysis times for the computationally efficient FSU were less than 1 minute, compared to 20 min for the fully deformable representation. As expected, each step in removing soft tissue structures resulted in reduced stiffness of the segment, with removal of anterior and posterior ligament structures coinciding with reduced stiffness in flexion-extension and axial rotation and removal of the intertransverse ligaments greatly reducing the stiffness of the segment in lateral bending. Removal of the facet capsular ligaments and facets resulted in significant reduction of the segment's stiffness in all motions. The ability of the model to accurately predict spine motion in response to an external load was quantified by calculating the RMS error between the model predicted

and experimentally measured torque-rotation and force-displacement behavior of the spine in all motions and sectioning steps. An RMS error of 0.0184 mm for force-displacement prediction in compression and an average RMS error of 0.114 degrees for torque-rotation prediction were found.

3.4 DISCUSSION

The computationally efficient FSU FE model developed here improves upon previous fully deformable and computationally efficient models in two primary areas. While models which include soft tissue structures are certainly useful when predicting stresses and strains in these structures, significantly reduced run times make the computationally efficient model more practical for clinical and design phase assessments. Previous computationally efficient models have used a ball and socket mechanical joint to provide the kinematic constraint between vertebrae. While this representation was successful at predicting torque-rotation behavior and reducing analysis time, it required translational degrees of freedom to be fixed. Although translations of vertebral bodies are relatively small compared to rotations, they are not negligible. Using a bushing rather than a ball and socket representation allows for stiffness in all 6 degrees of freedom to be accounted for, resulting in a more accurate prediction of spine motion.

Biomechanical testing with the soft tissue sectioning protocol made it possible to tune the bushing to represent the FSU with varying levels of intact soft tissue structures. This allows understanding and quantification of the contributions of specific structures to the mechanical stability of the segment. It is also common for certain structures to be

removed to enable placement of a device. Having the ability to vary the stiffness of the model depending on what structures have been resected for device placement will make the model better suited to predict device performance.

Table 3.1 FSU testing protocol. Hybrid loading indicates the FSU was loaded until the maximum angle from the intact case was reached.

Test Description	**Test Performed**
Intact	FE, LB, AR (± 10Nm)
Section Supraspinous Lig.	FE, AR (Hybrid)
Section Interspinous Lig.	FE, AR (Hybrid)
Section Posterior Longitudinal Lig.	FE, AR (Hybrid)
Section Anterior Longitudinal Lig.	FE, AR (Hybrid)
Section Intertransverse Lig.	LB, AR (Hybrid)
Section Facet Capsules	FE, LB, AR (Hybrid)
Remove Facets	FE, LB, AR, Comp. (Hybrid)

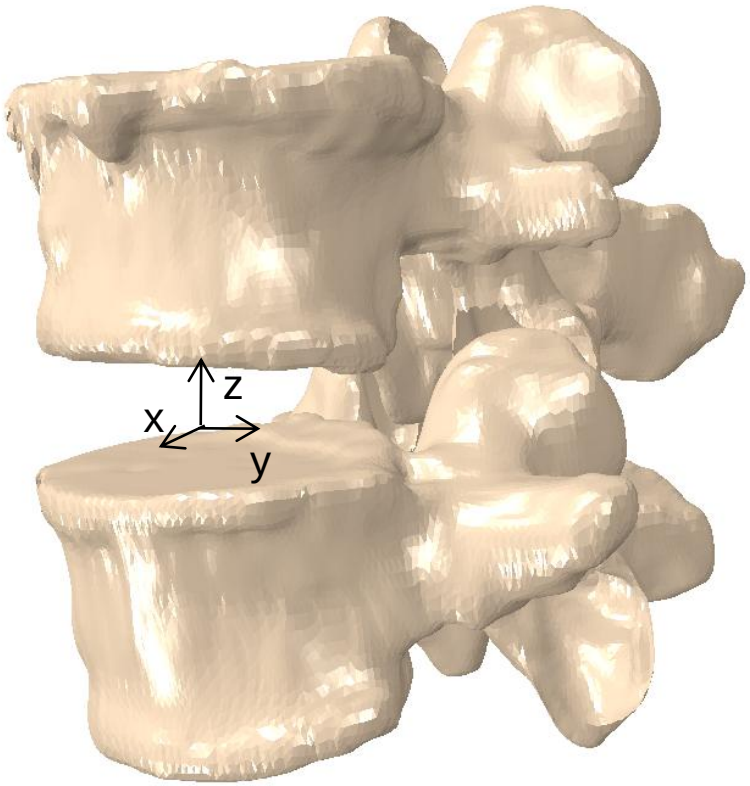

Figure 3.1 Computationally efficient L4-L5 FSU model with bushing connector element representation for constraints of soft tissues.

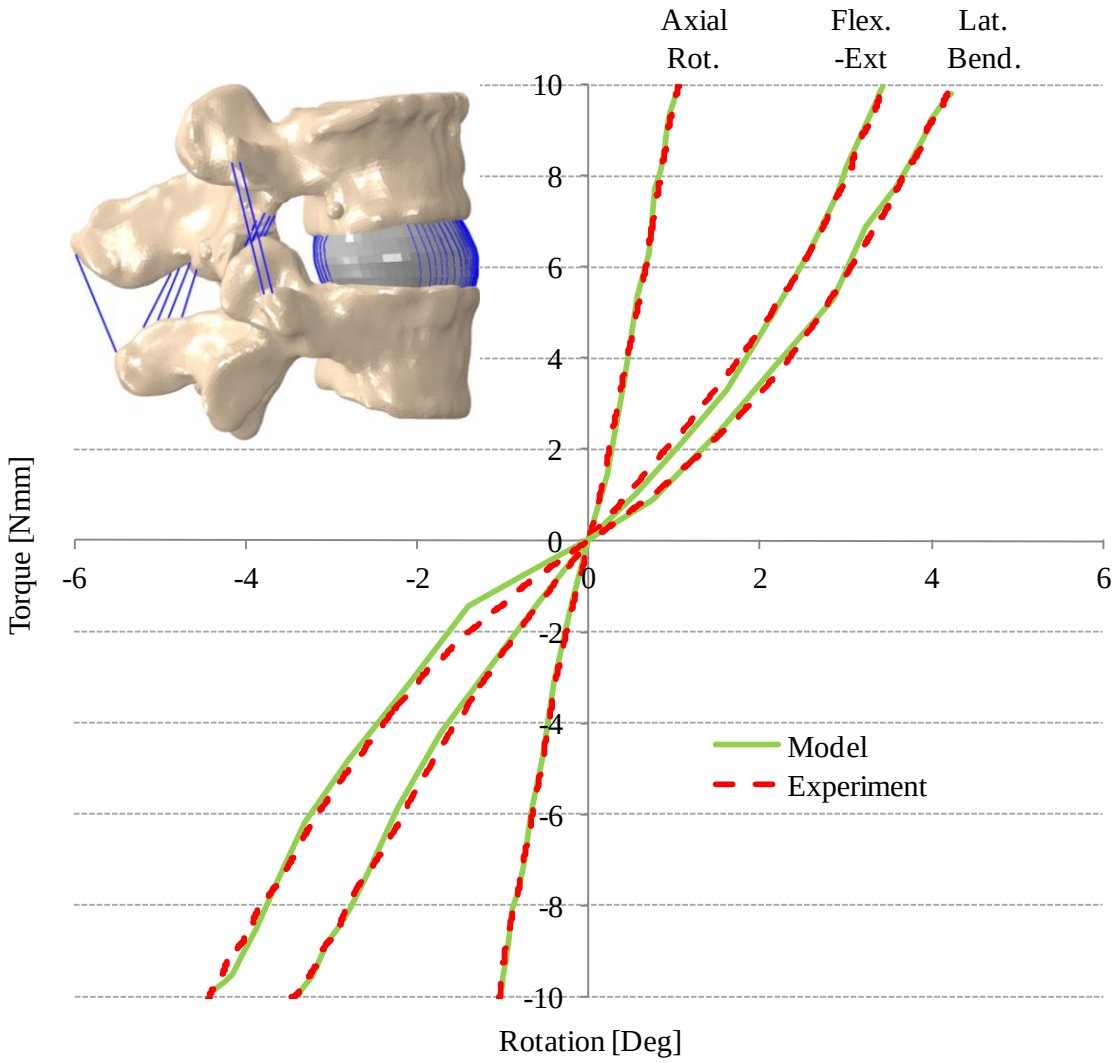

Figure 3.2 Comparison of model predicted and experimentally measured torque-rotation response of the intact L4-L5 FSU in flexion-extension, lateral bending, and axial rotation.

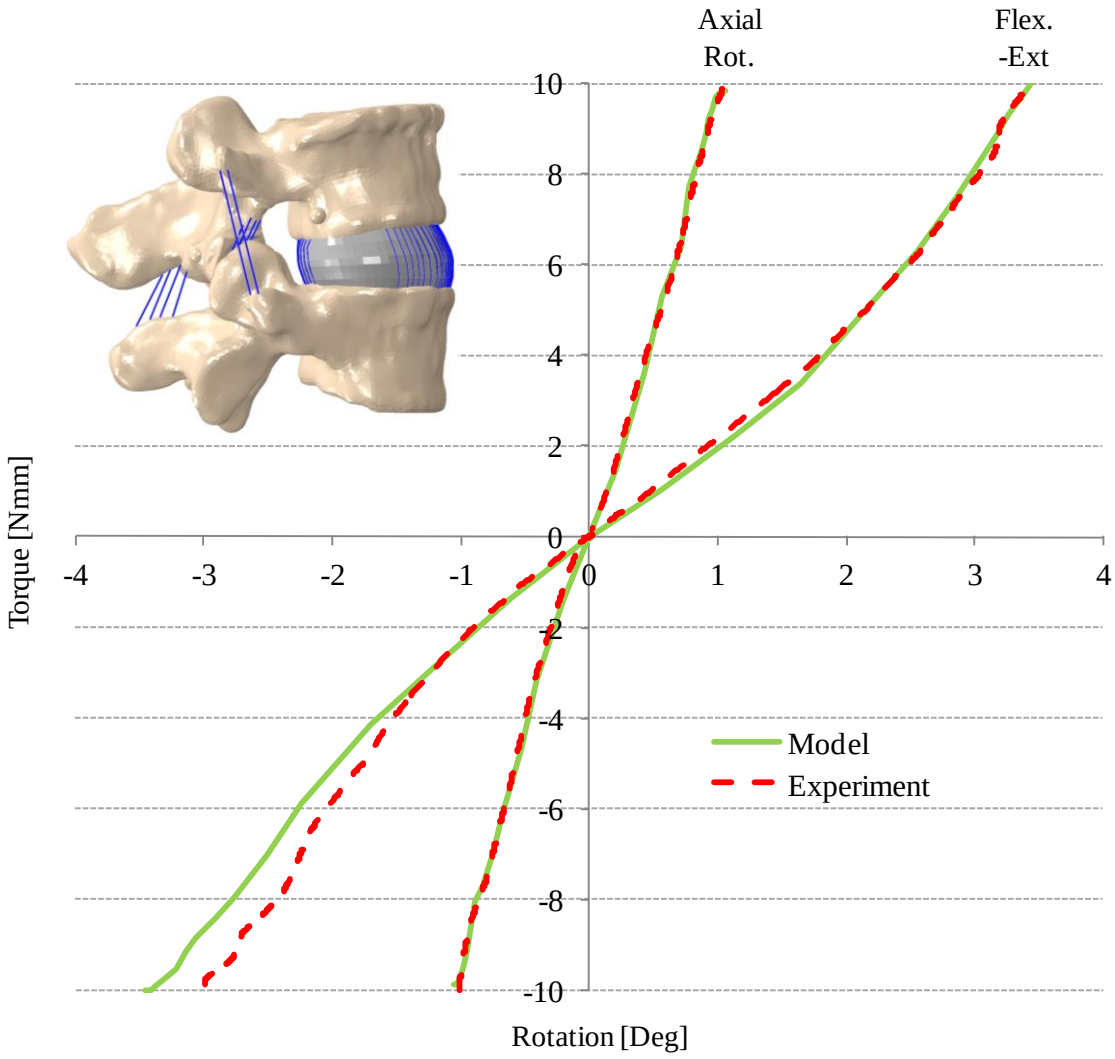

Figure 3.3 Comparison of model predicted and experimentally measured torque-rotation response of the L4-L5 FSU in flexion-extension and axial rotation following resection of the supraspinous ligament.

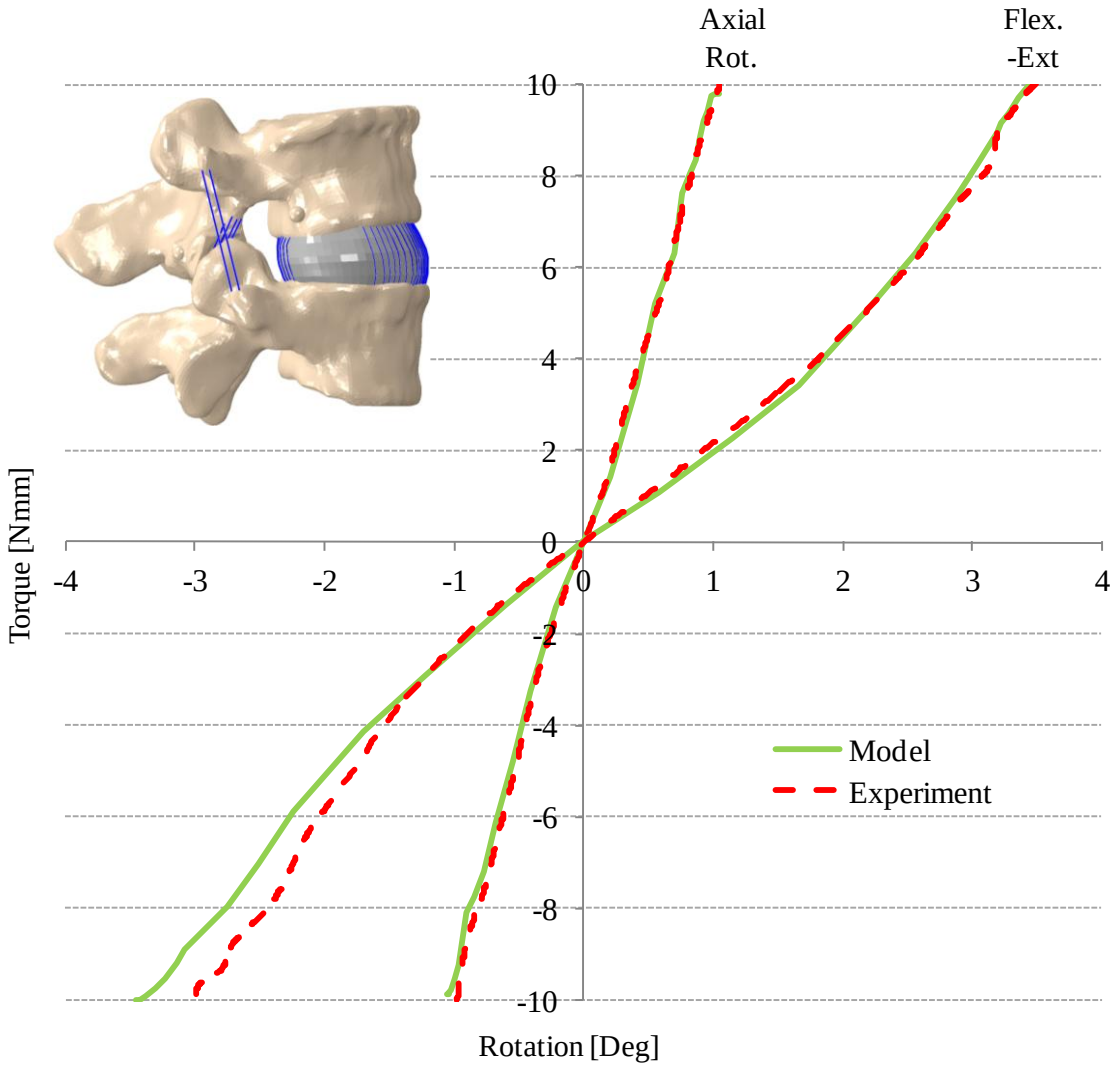

Figure 3.4 Comparison of model predicted and experimentally measured torque-rotation response of the L4-L5 FSU in flexion-extension and axial rotation following resection of the supraspinous and interspinous ligaments.

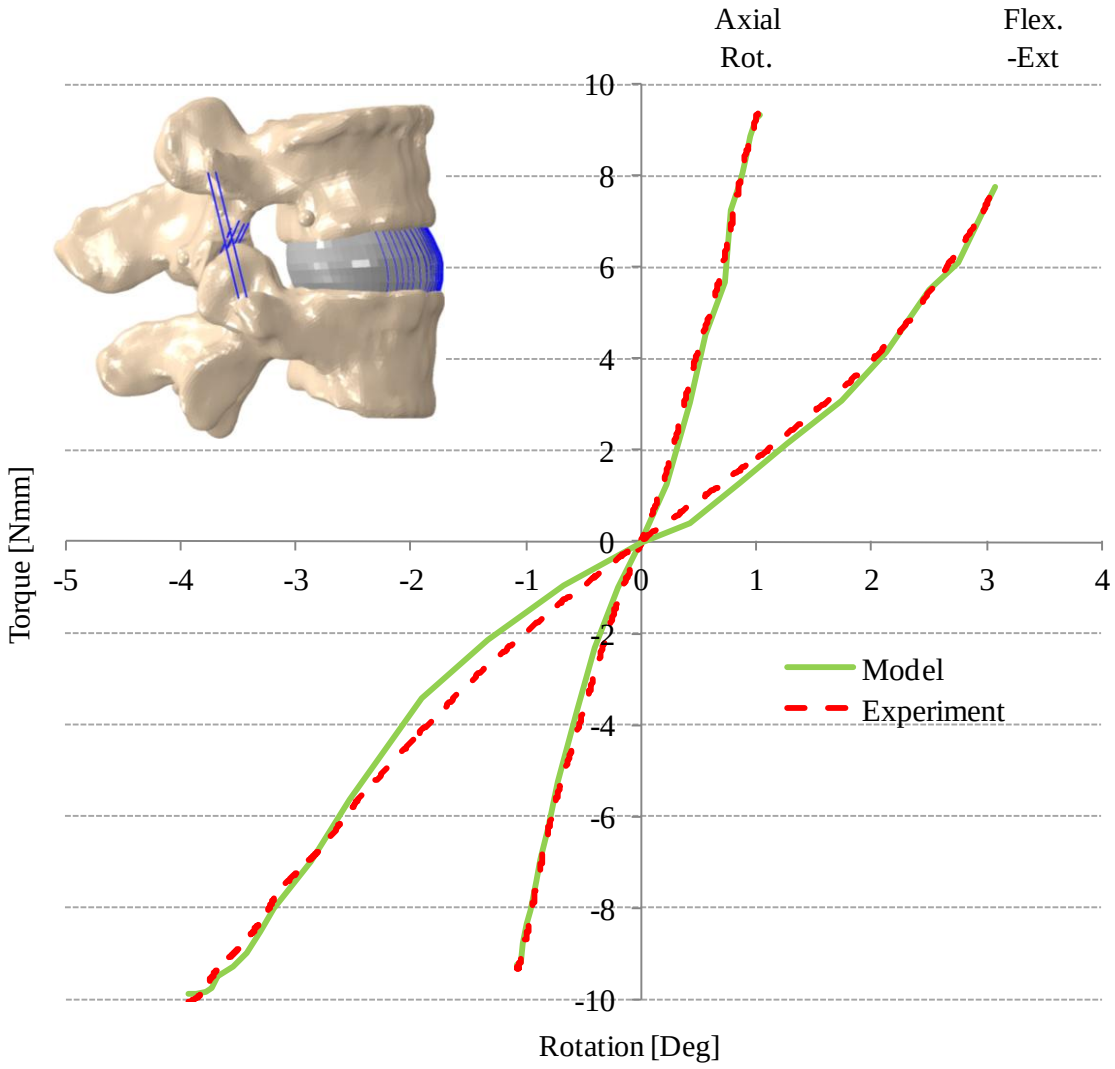

Figure 3.5 Comparison of model predicted and experimentally measured torque-rotation response of the L4-L5 FSU in flexion-extension and axial rotation following resection of the supraspinous, interspinous, and posterior longitudinal ligaments.

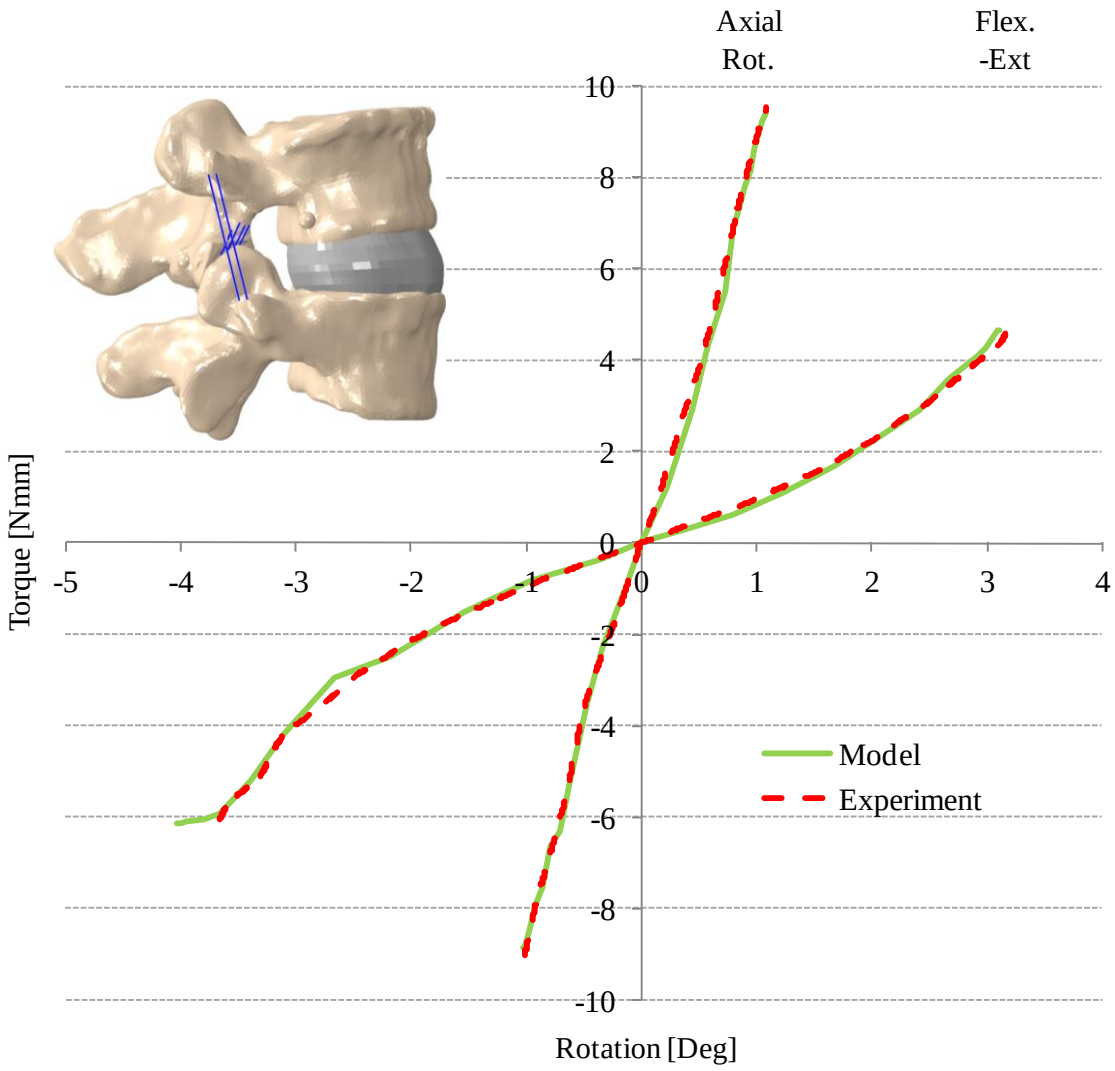

Figure 3.6 Comparison of model predicted and experimentally measured torque-rotation response of the L4-L5 FSU in flexion-extension and axial rotation following resection of the supraspinous, interspinous, posterior longitudinal, and anterior longitudinal ligaments.

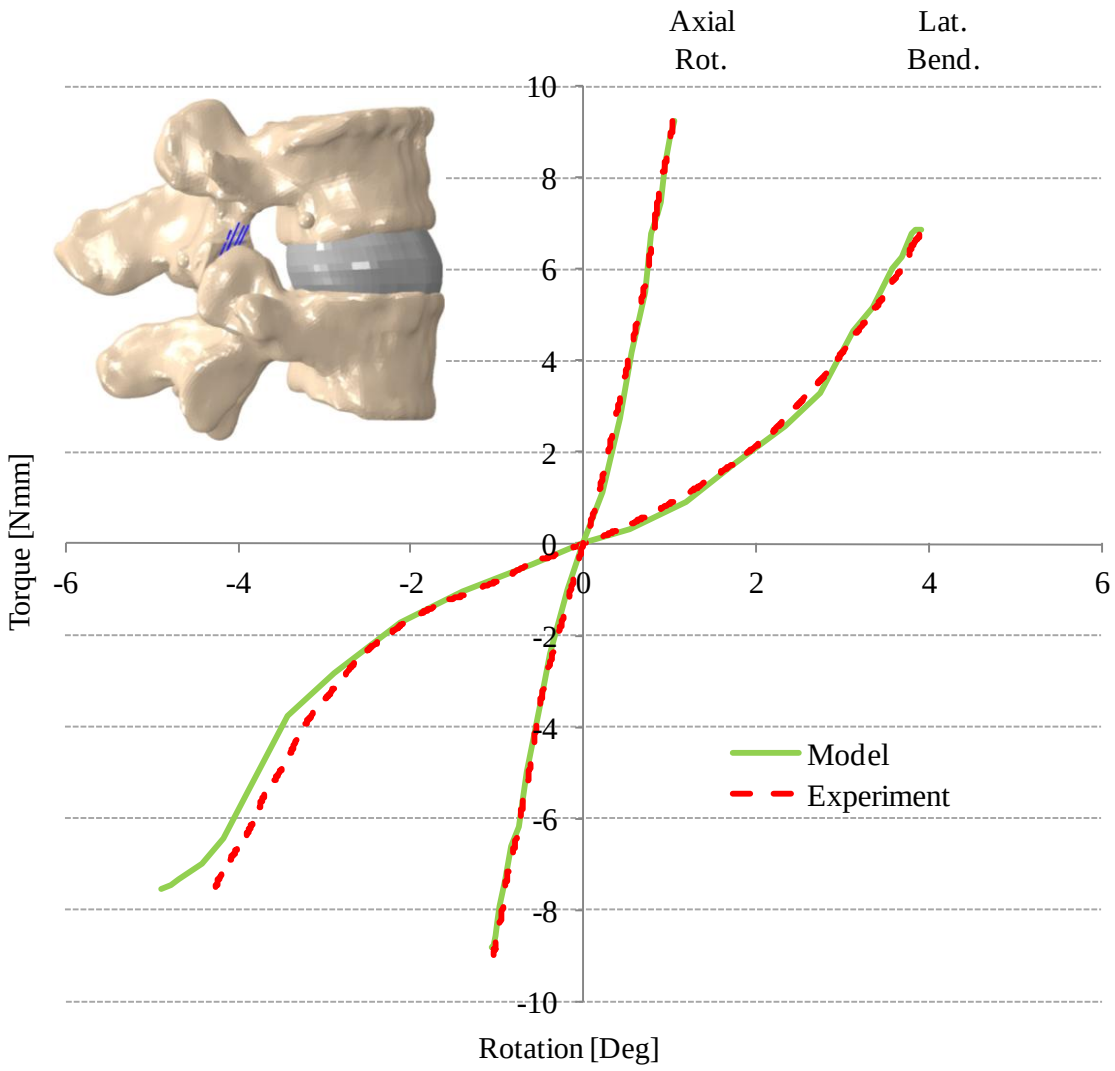

Figure 3.7 Comparison of model predicted and experimentally measured torque-rotation response of the L4-L5 FSU in axial rotation and lateral bending following resection of the supraspinous, interspinous, posterior longitudinal, anterior longitudinal, and intertransverse ligaments.

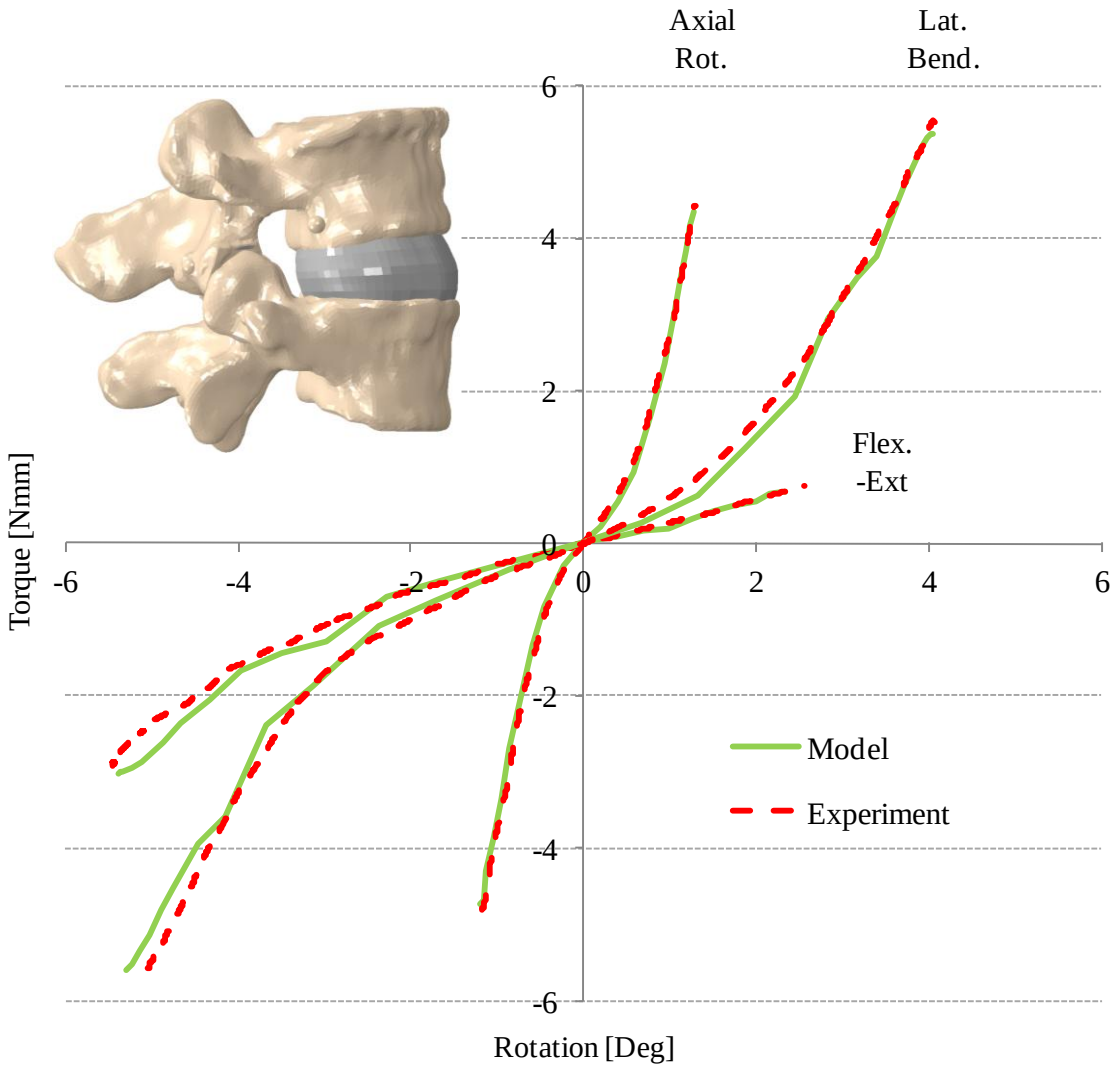

Figure 3.8 Comparison of model predicted and experimentally measured torque-rotation response of the L4-L5 FSU in flexion-extension, axial rotation and lateral bending following resection of the supraspinous, interspinous, posterior longitudinal, anterior longitudinal, intertransverse, and facet capsular ligaments.

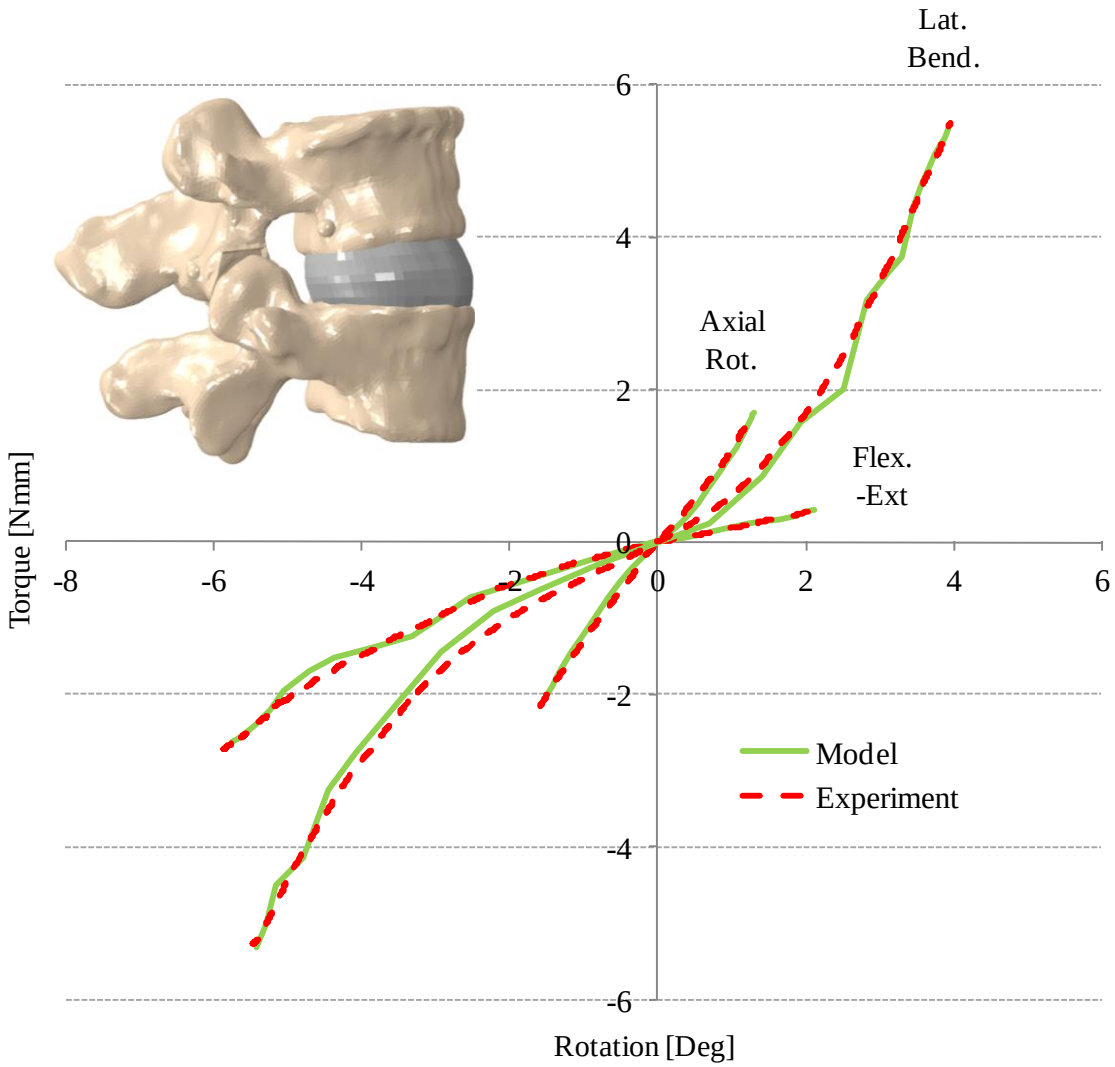

Figure 3.9 Comparison of model predicted and experimentally measured torque-rotation response of the L4-L5 FSU in flexion-extension, axial rotation and lateral bending following resection of the supraspinous, interspinous, posterior longitudinal, anterior longitudinal, intertransverse, and facet capsular ligaments, as well as the facet joints.

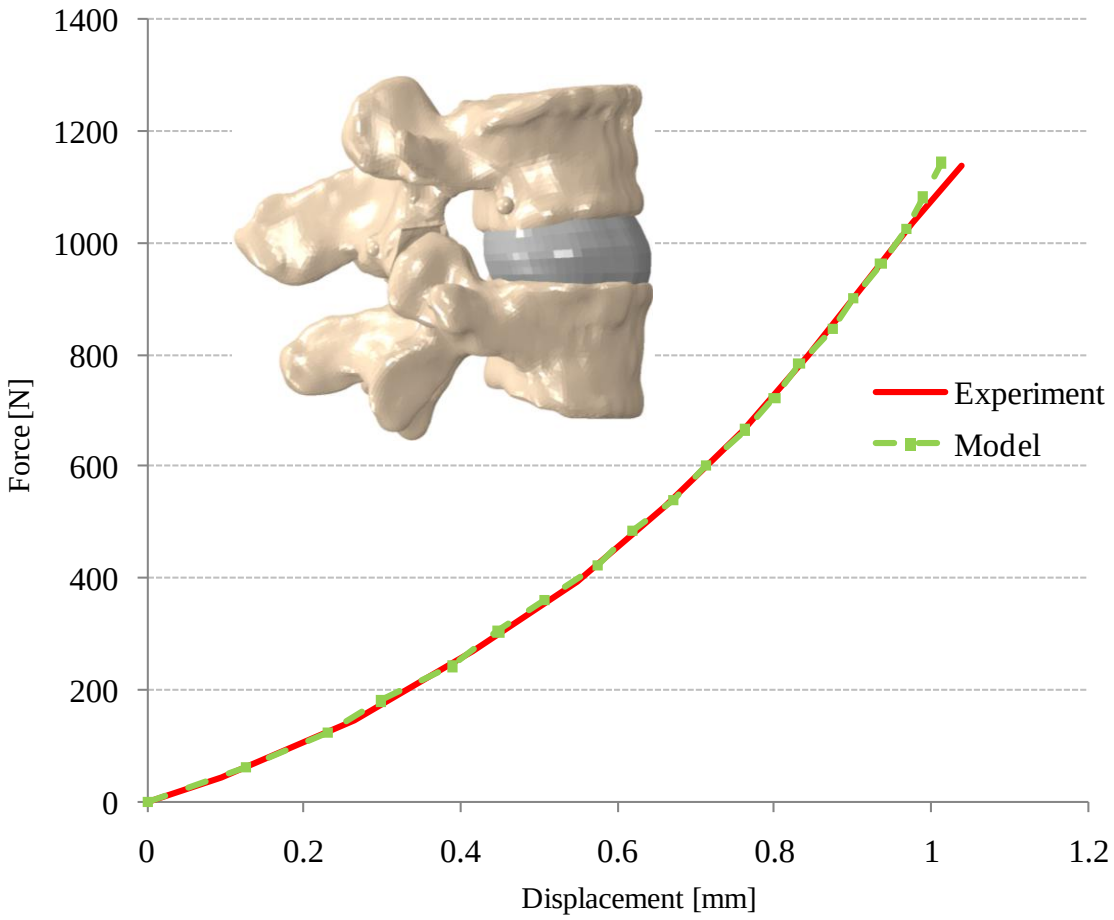

Figure 3.10 Comparison of model predicted and experimentally measured force-displacement response of the L4-L5 FSU in axial compression following resection of the supraspinous, interspinous, posterior longitudinal, anterior longitudinal, intertransverse, and facet capsular ligaments, as well as the facet joints.

Table 3.2 RMS values between model predicted and experimentally measured torque-rotation and force-displacement behavior of the L4-L5 FSU.

Sectioning Step	Motion	RMS (degrees)
1	FE	0.083799
1	LB	0.060263
1	AR	0.018729
2	FE	0.293634
2	AR	0.025586
3	FE	0.295072
3	AR	0.054081
4	FE	0.0454
4	AR	0.031589
5	FE	0.219695
5	AR	0.024883
6	FE	0.311331
6	AR	0.023547
7	FE	0.117389
7	AR	0.051712
7	LB	0.227654
8	FE	0.146926
8	AR	0.081933
8	LB	0.052971
8	Compression	0.018402 (mm)

CHAPTER 4 – TUNING OF FINITE ELEMENT MODEL – PREDICTED MULTI-SEGMENT KINEMATICS

4.1 INTRODUCTION

Although multi-segment models will have increased run times compared to FSU models, the use of bushing connector elements to represent the soft tissue kinematic constraints increases computational efficiency enough that these models can be useful for clinical and design phase assessments. As is so commonly presented in the literature, the prevalence of adjacent segment degeneration (ASD) following instrumentation of a degenerated segment has made the study of the adjacent segments mechanics a point of high interest. The primary advantage of a lumbar model consisting of multiple levels is the ability to evaluate device performance and changes in spine mechanics at both the implanted level and adjacent segments. The multi-segment model can also be converted into a musculoskeletal model with the addition of the lumbar musculature. The reduced analysis times of the computationally efficient model makes it ideal for optimization of muscle parameters, which requires quickly running multiple simulations.

Multi-segment lumbar models vary from consisting of 3 vertebrae to all 5 lumbar vertebrae and the sacrum. In this study, the development and validation of an L1-S1 model is presented. Simulations can be run to assess device performance and spine

mechanics at all levels, including the L5-S1 level, which is a common treatment level often neglected in computational models.

4.2 METHODS

4.2.1 Experiment Kinematic Analysis

Development and validation of the FE L5-S1 multi-segment model was possible due to prior experimental testing of the cadaver specimen at the University of Washington's Applied Biomechanics Lab. Before reducing the specimens to FSUs, testing was performed on the lumbar spines consisting of the 5 lumbar vertebrae and the sacrum. The specimen used for this model had mild to moderate degeneration, which was determined with x-ray screening. All surrounding soft tissues other than the osteoligamentous structures and disc were removed. Recording of the vertebral body kinematics was consistent with the procedure described in the FSU kinematic analysis procedure. Four radio-opaque marker beads that were 4mm in diameter were embedded into each vertebral body and fixed with cyanoacrylate glue. High resolution computed tomography (CT) scans were obtained for the specimen so that the geometry could later be reconstructed and the vertebral kinematics could be applied to the reconstructed markers. Screws were placed in the ends of L1 and the sacrum and the vertebral bodies were potted in poly-methylmethacrylate. Pure moment testing of the lumbar segment was performed using the Applied Biomechanics Lab's custom multi-axis spine motion simulator. The specimens were evaluated with all soft tissues intact, subject to pure moment loading (flexion, extension, lateral bending, and axial rotation), and combination

loading (flexion/extension + lateral bending, flexion/extension + axial rotation, lateral bending + axial rotation), while segment motion was recorded using a 4 camera motion capture system. Pure moments of 10 Nm for single axis loading and 7 Nm for multi-axis loading were applied to the cephalad end and the caudal end was fixed to a 6-axis load cell to collect force and moment data that was transmitted through the spine.

4.2.2 L1-S1 Multi-Segment Finite Element Model

A specimen specific L1-S1 multi-segment FE model was developed in Abaqus/Explicit (Simulia, Providence, RI) from high-resolution computed tomography scans of an adult cadaveric spine. The spine was that of a 71 year old male who was 68" tall and weighed 267 lbs. The spine was considered to be mild to moderately degenerated with a disc grade of 3-4. The scans were imported in to ScanIP (Simpleware, Exeter, UK) as dicom files and the spinal geometry was reconstructed manually by selecting the bone portion of each image. The reconstructed geometry consisted of vertebral bodies L1 through L5 and the sacrum. These geometries were brought in to Hypermesh (Altair, Troy, MI) for mesh generation. The vertebrae were represented as rigid bodies and were meshed with 3 node triangular shell elements. All soft tissue structures such as the ligaments, intervertebral disc, and facet cartilage were excluded from the model. A 6 degree of freedom bushing connector element was placed between each adjacent vertebrae at a point equidistant from the superior and inferior endplates and centered in the medial-lateral and anterior-posterior directions. The stiffness of these connector elements were responsible for providing the appropriate torque-rotation and force-

displacement constraint in the absence of the soft tissue structures. Nonlinear stiffness curves were defined for each degree of freedom for the connector element and properties were optimized to reproduce the kinematic-moment measured response from experiment. The bushing connector consists of 2 coincident nodes placed between vertebrae. One of the nodes is beamed to the rigid body reference node of the inferior vertebrae the other is beamed to the rigid body reference node of the superior vertebrae. A dummy element was defined with bone properties for calculation of increment size within the explicit solver.

4.2.3 Computational Kinematic Analysis

Validation of the L1-S1 multi-segment model was based on torque-rotation and force-displacement data obtained from the biomechanical testing of this cadaver specimen at the University of Washington's Applied Biomechanics Lab. Fiducial marker positions were extracted from the CT scans at the time the bone geometries were reconstructed. The kinematic data collected on the vertebral segment motion with the Vicon motion capture system during experimental testing was used to control the motion of the segment in flexion, extension, lateral bending, axial rotation, and combined motions. The sacrum was constrained in all degrees of freedom and displacements of the fiducial markers were used to recreate the motion experienced in experimental testing. Reaction moments at the fixed rigid body reference node of the sacrum and rotations at each of the rigid body reference nodes of the vertebrae were requested as outputs from the simulation and compared to the torque-rotation response measured in experiment. Translational degree of freedom stiffness calculated during the intact FSU tuning were

applied to the multi-segment model. Optimization of the bushing stiffness properties was performed in Isight (Simulia, Providence, RI) using adaptive simulated annealing. The objective function that was minimized was the sum y-squared difference between the model predicted and experimentally measured torque-rotation response at each level of the multi-segment specimen in flexion, extension, lateral bending, and axial rotation, while the stiffness parameters were allowed to vary.

4.3 RESULTS

The computationally efficient multi-segment model effectively predicted the spine segment motion while also significantly reducing the analysis time compared to the fully deformable model. Torque-rotation behavior for the optimized multi-segment model agreed well with the experiment in flexion, extension, lateral bending, and axial rotation. Overlays of the force controlled and marker-displacement controlled models demonstrate the ability of the model to represent the motion of the spine segment in its entirety, and not only accurately reproduce the torque-rotation behavior of the segment. Analysis times for the computationally efficient multi-segment model were just over 2 minutes, compared to 3 hours for the fully deformable representation. Overlays of the marker-displacement controlled model and force controlled model during combined loading demonstrate the models ability to effectively reproduce more complex motions. The ability of the model to accurately predict spine motion in response to an external load was quantified by calculating the RMS error between the model predicted and experimentally

measured torque-rotation behavior of the spine in all motions and levels. The average RMS error was 0.0448 degrees.

4.4 DISCUSSION

As demonstrated by the results, the computationally efficient L1-S1 multi-segment model can accurately predict the kinematics of the spine segment in response to an external load. The model will be useful in multiple applications, such as prediction of healthy and instrumented spine mechanics and evaluation of device performance. Although the inclusion of multiple levels results in a longer analysis time than the FSU, there are several advantages that the multi-segment model presents.

When studying the effects of device inclusion, evaluation of the device's performance is not limited to the instrumented level. The ability to study changes in mechanics at all levels will help address the causes of adjacent segment degeneration. Additionally, the FE modeling platform is very versatile, and makes it possible to convert the efficient fully rigid model into a hybrid rigid/deformable model that incorporates both computationally efficient and deformable levels. This makes it possible to study the mechanics of deformable structures at a specified level, while still saving significant computational analysis time.

Most models simulate motion through the application of external loads such as pure moments. Although this method is an accepted practice, musculoskeletal models are able to simulate loading that is physiologically more accurate and consistent with in vivo conditions. The model's computationally efficiency will be very useful in efforts to

develop a lumbar musculoskeletal model. The model's short analysis time is ideal for optimization of muscle parameters, which will require multiple analyses to be run.

Table 4.1 Multi-segment testing protocol.

Motion	Moment
FE	±10Nm
LB	±10Nm
AR	±10Nm
FE + LBR	±7Nm FE ±7Nm LB
FE + LBL	±7Nm FE ±7Nm LB
FE + AR	±7Nm FE ±7Nm AR
LB + AR	±7Nm LB ±7Nm AR

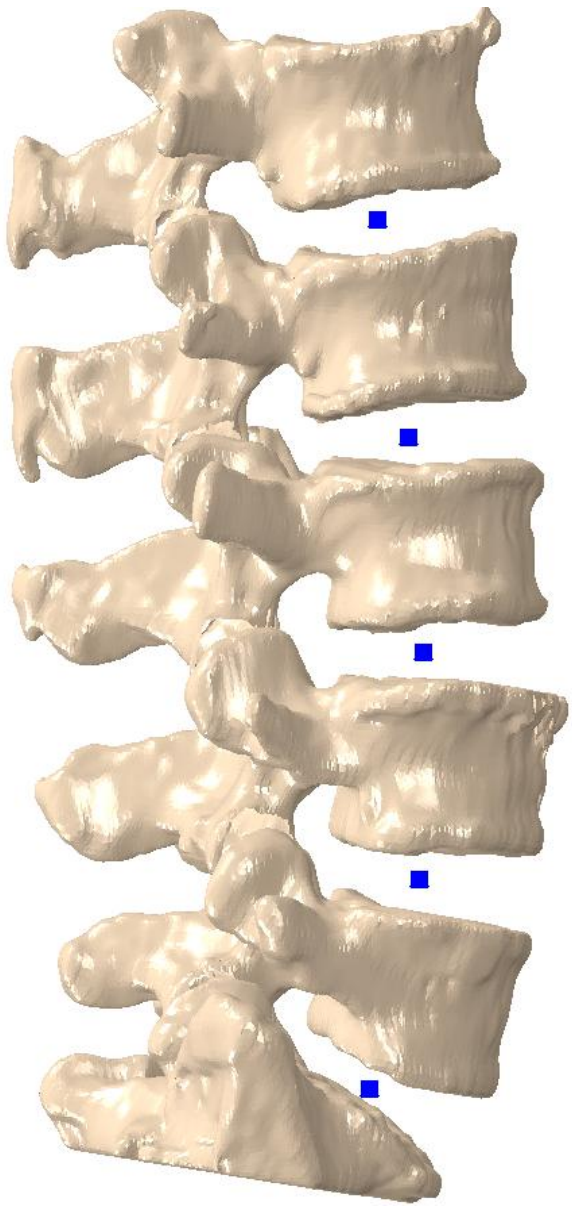

Figure 4.1 Computationally efficient L1-S1 multi-segment model with bushing connector representation for soft tissue constraint.

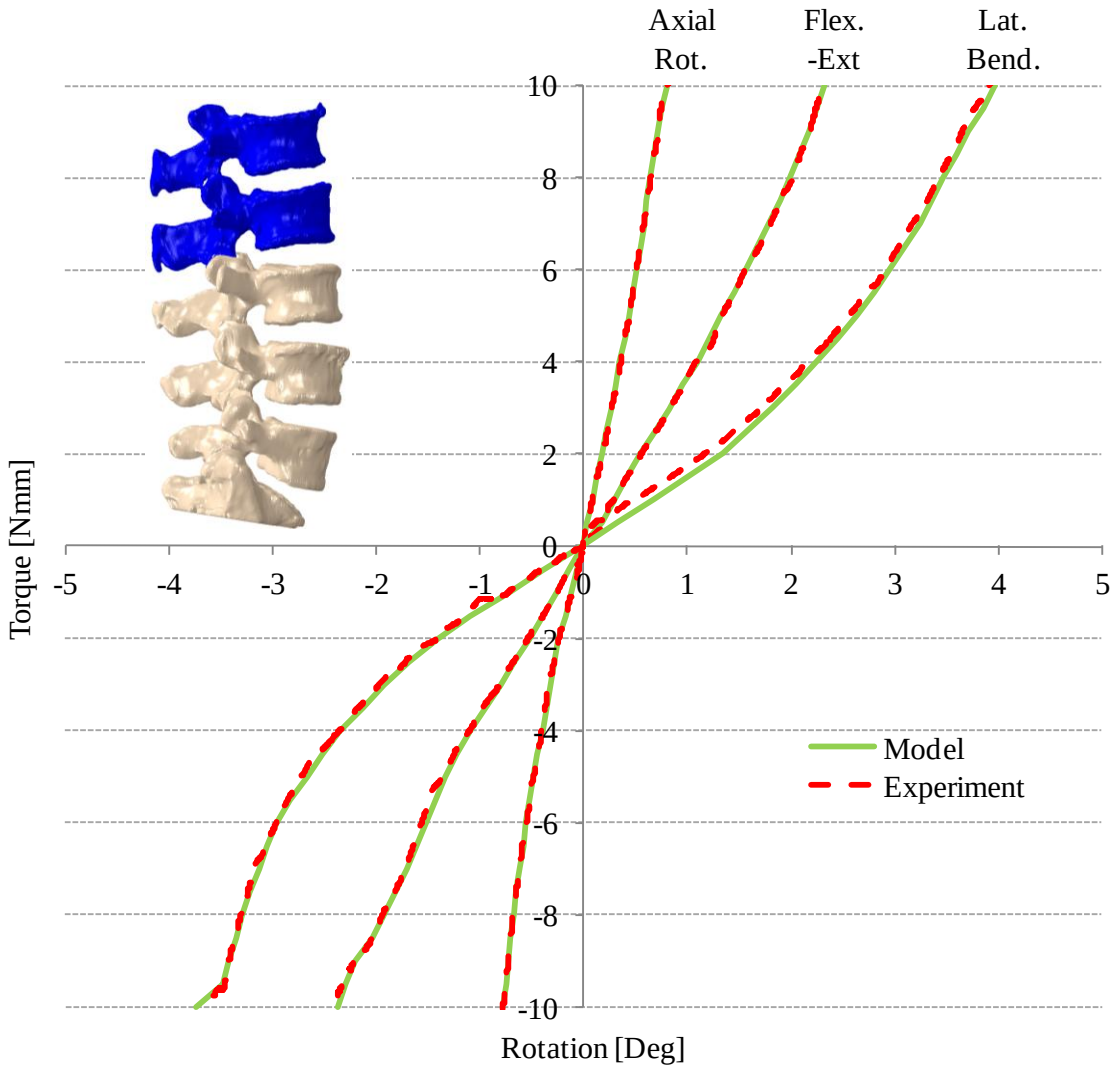

Figure 4.2 Comparison of model predicted and experimentally measured torque-rotation response of the intact L1-S1 multi-segment spine at level L1-L2 in flexion-extension, lateral bending, and axial rotation.

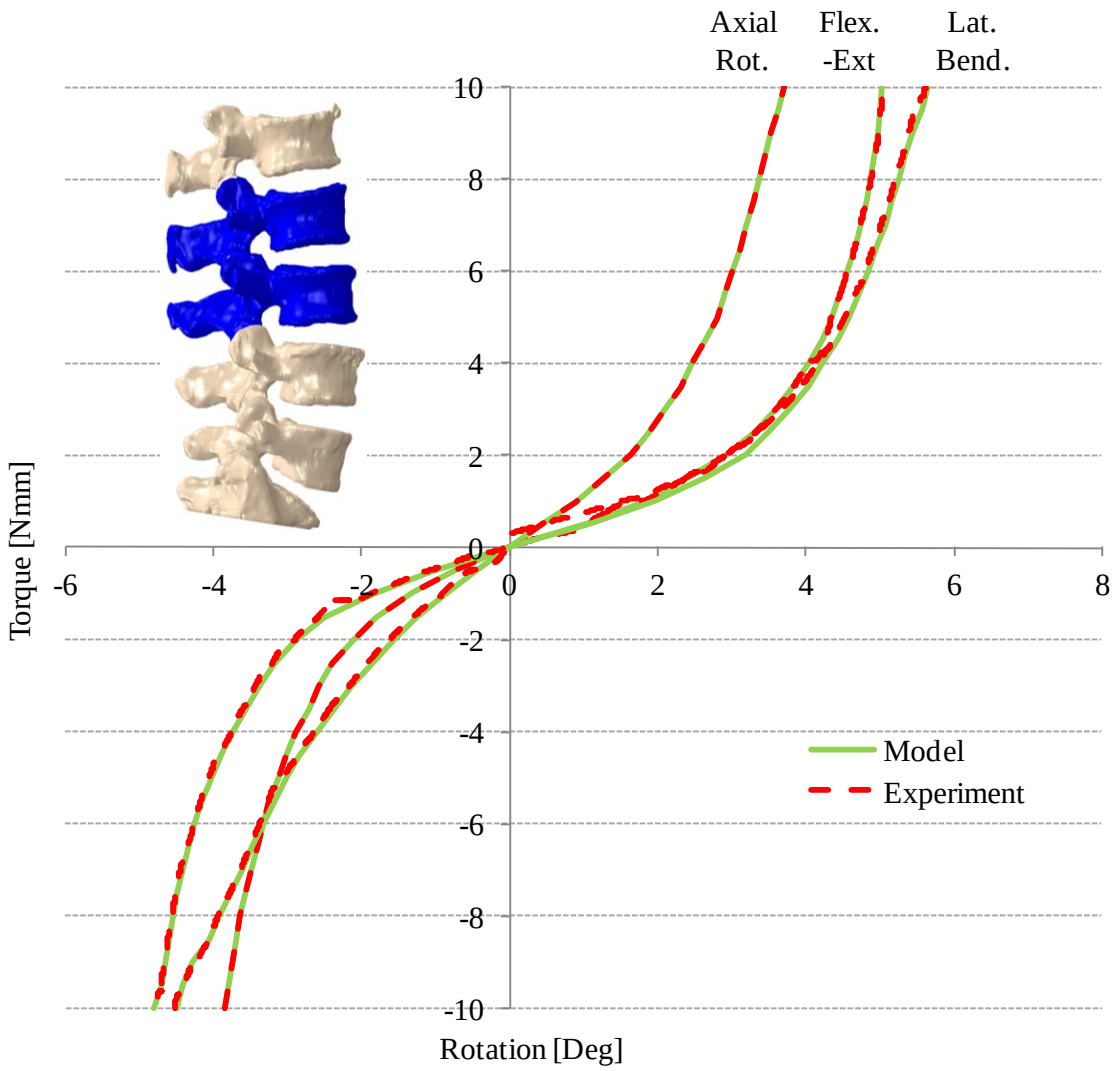

Figure 4.3 Comparison of model predicted and experimentally measured torque-rotation response of the intact L1-S1 multi-segment spine at level L2-L3 in flexion-extension, lateral bending, and axial rotation.

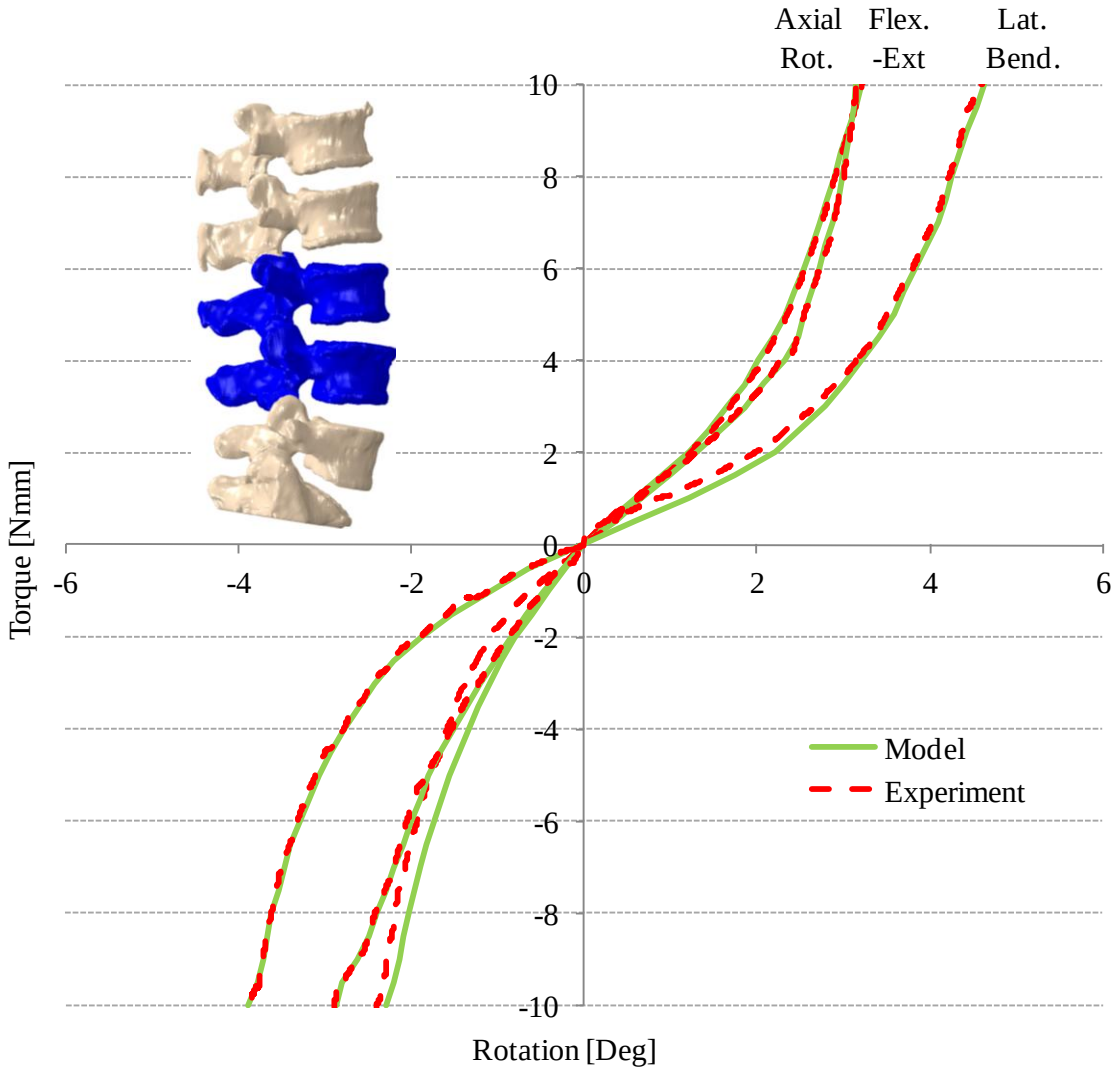

Figure 4.4 Comparison of model predicted and experimentally measured torque-rotation response of the intact L1-S1 multi-segment spine at level L3-L4 in flexion-extension, lateral bending, and axial rotation.

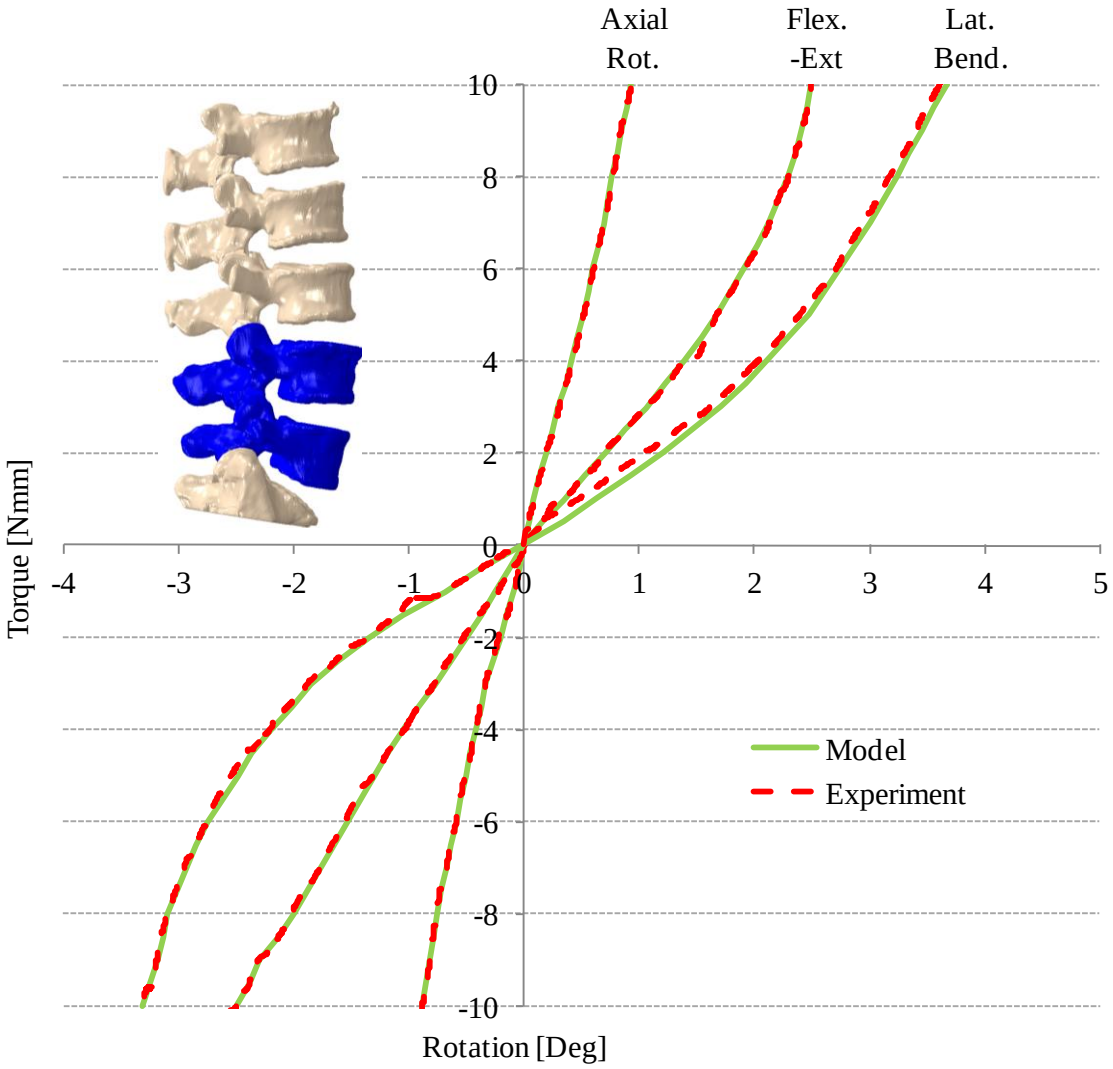

Figure 4.5 Comparison of model predicted and experimentally measured torque-rotation response of the intact L1-S1 multi-segment spine at level L4-L5 in flexion-extension, lateral bending, and axial rotation.

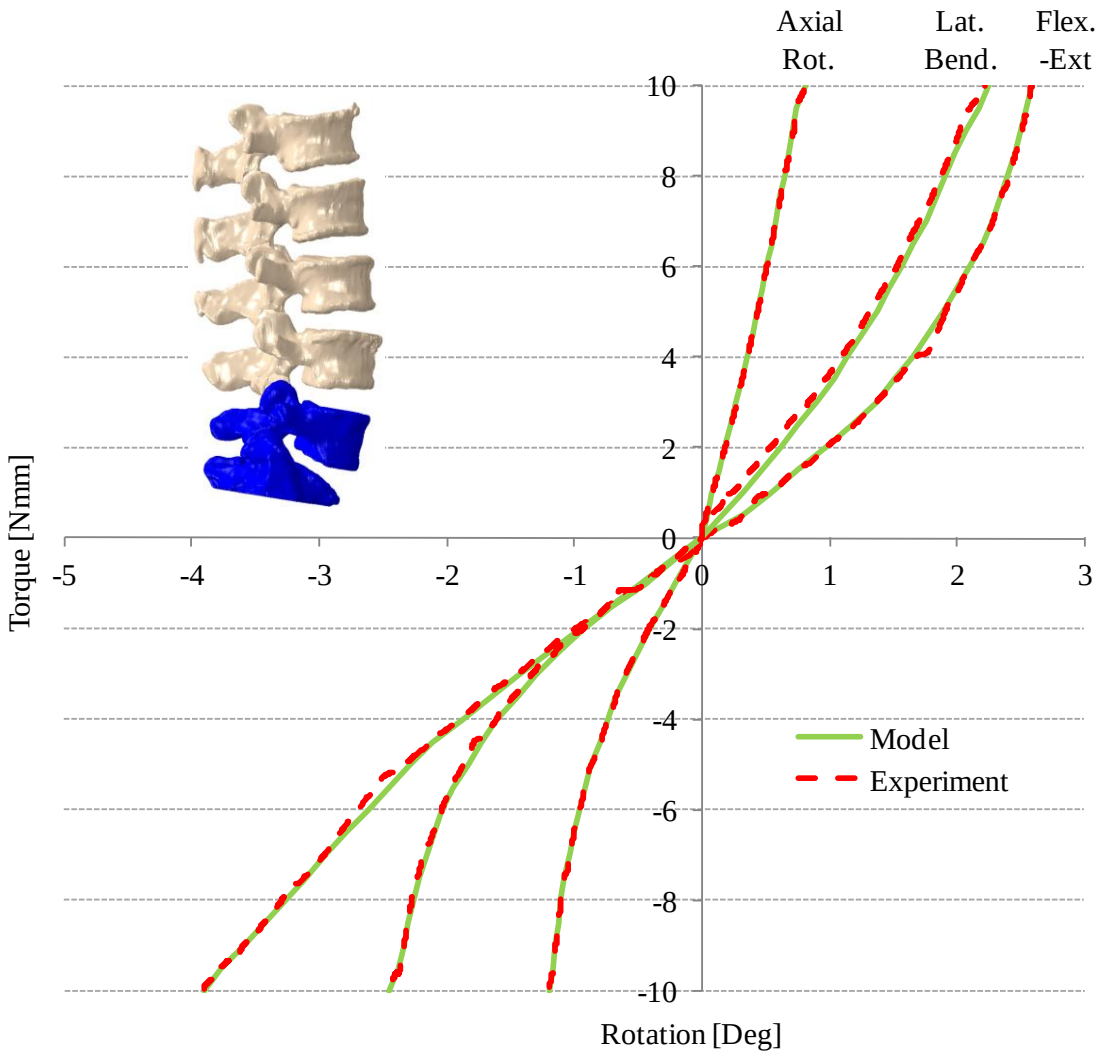

Figure 4.6 Comparison of model predicted and experimentally measured torque-rotation response of the intact L1-S1 multi-segment spine at level L5-S1 in flexion-extension, lateral bending, and axial rotation.

Table 4.2 RMS values between model predicted and experimentally measured torque-rotation behavior of the L1-S1 multi-segment model.

Level	Motion	RMS (degrees)
L1-L2	FE	0.016922
L1-L2	LB	0.087658
L1-L2	AR	0.004444
L2-L3	FE	0.032354
L2-L3	LB	0.087973
L2-L3	AR	0.02643
L3-L4	FE	0.029359
L3-L4	LB	0.078837
L3-L4	AR	0.147671
L4-L5	FE	0.013128
L4-L5	LB	0.069353
L4-L5	AR	0.007803
L5-S1	FE	0.028871
L5-S1	LB	0.037254
L5-S1	AR	0.003999

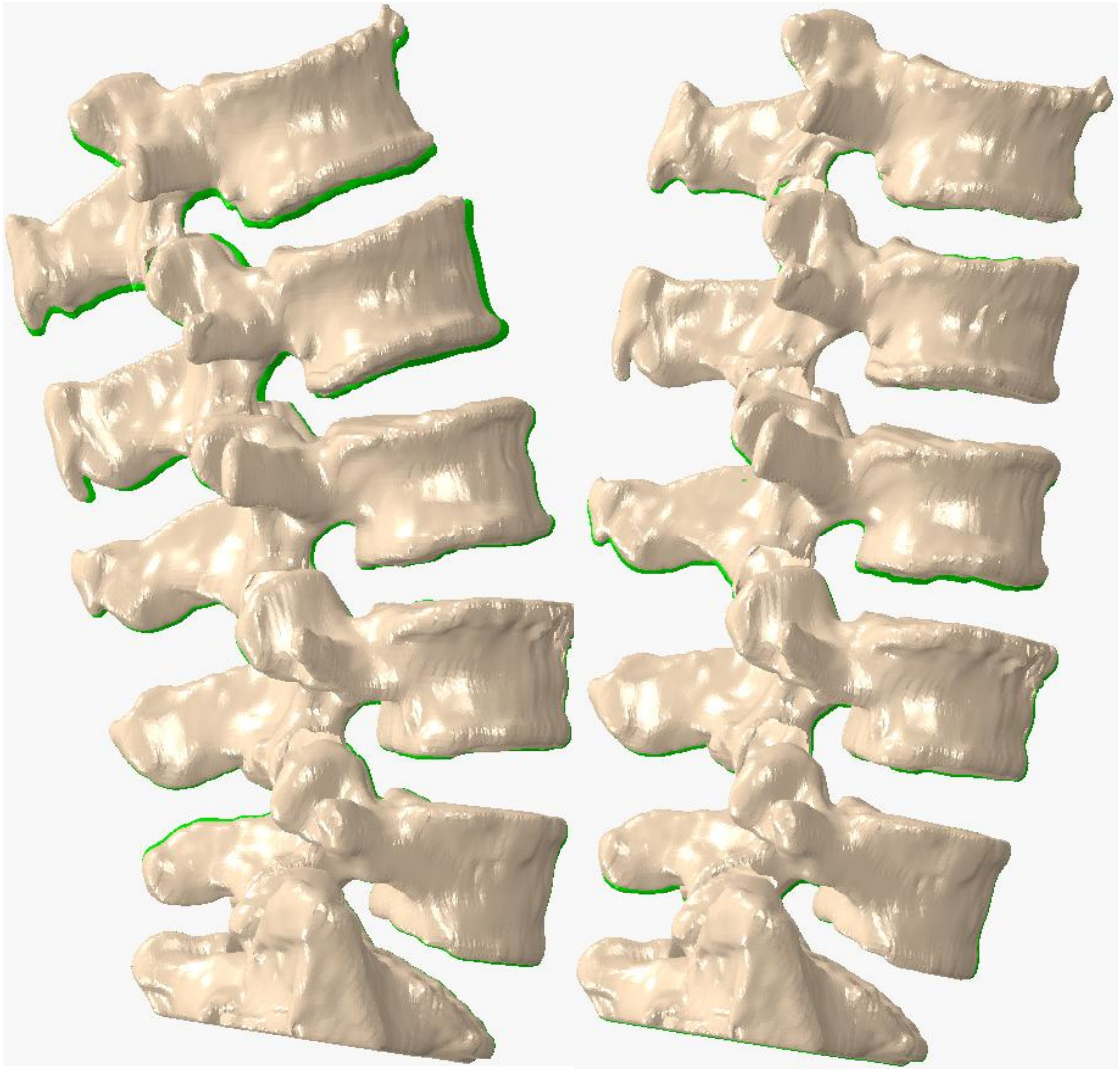

Figure 4.7 Overlay comparison of marker-displacement controlled model (green) and force controlled model in extension (left) and flexion (right).

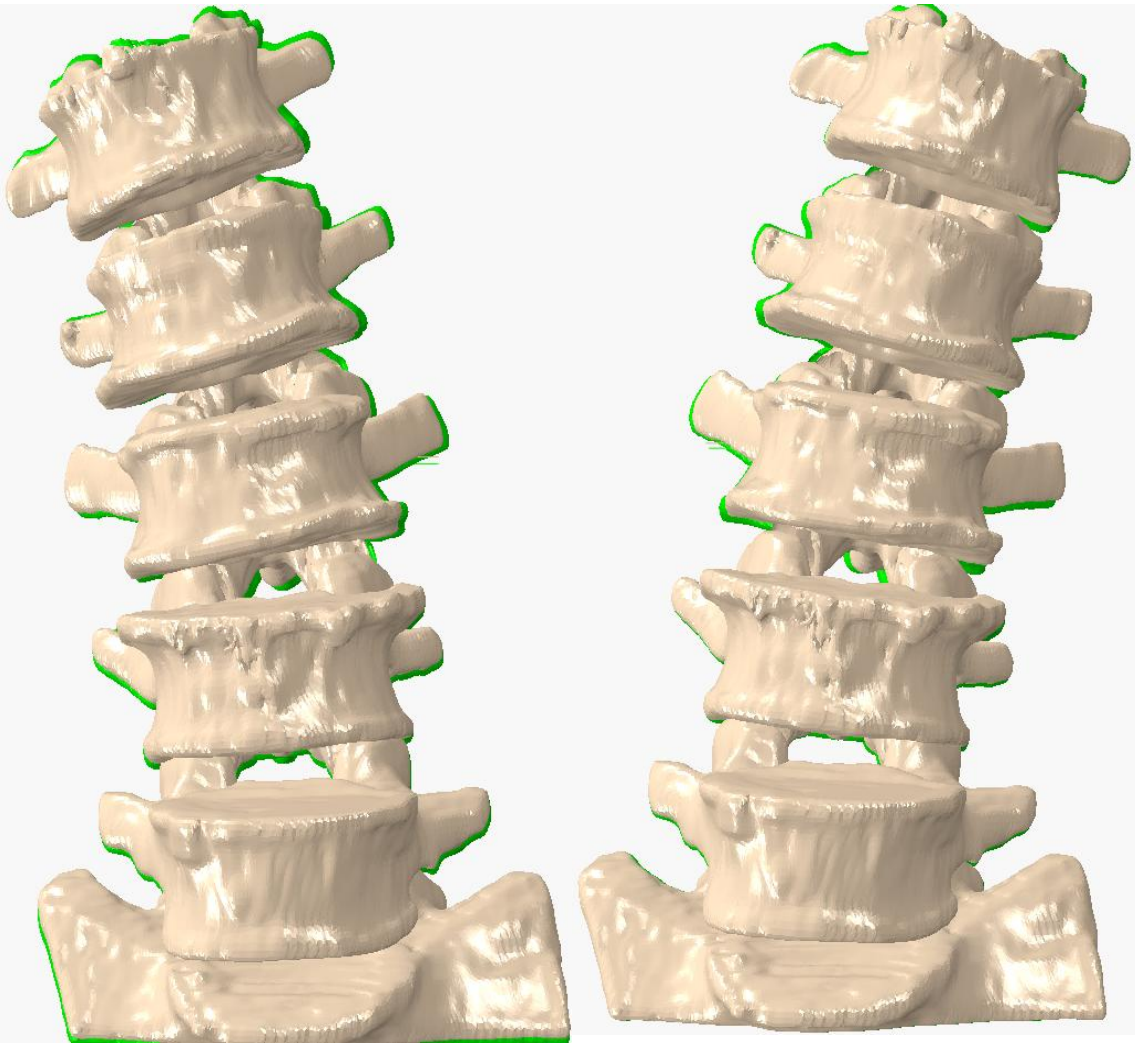

Figure 4.8 Overlay comparison of marker-displacement controlled model (green) and force controlled model in right lateral bend (left) and left lateral bend (right).

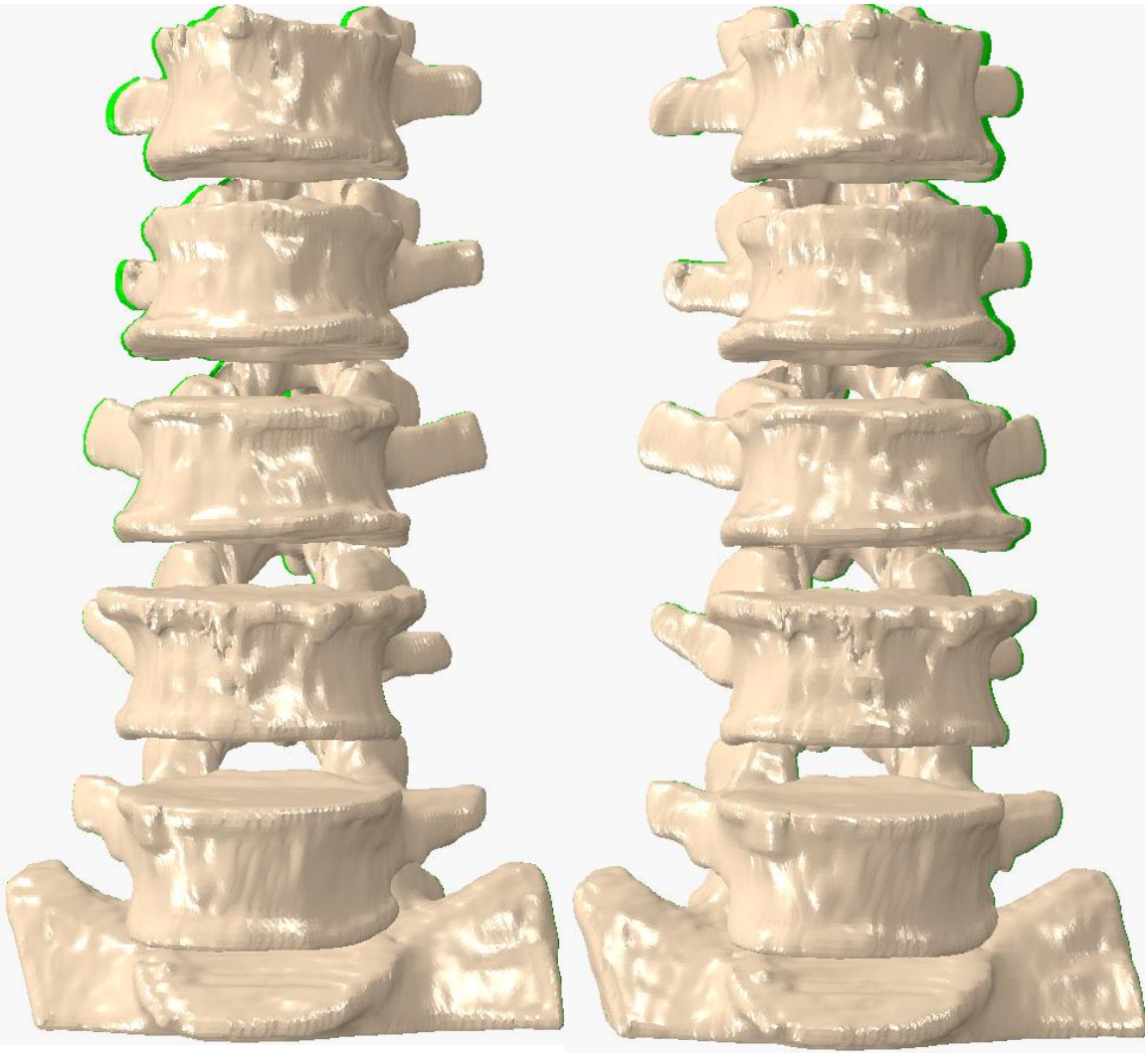

Figure 4.9 Overlay comparison of marker-displacement controlled model (green) and force controlled model in clockwise axial rotation (left) and counterclockwise axial rotation (right).

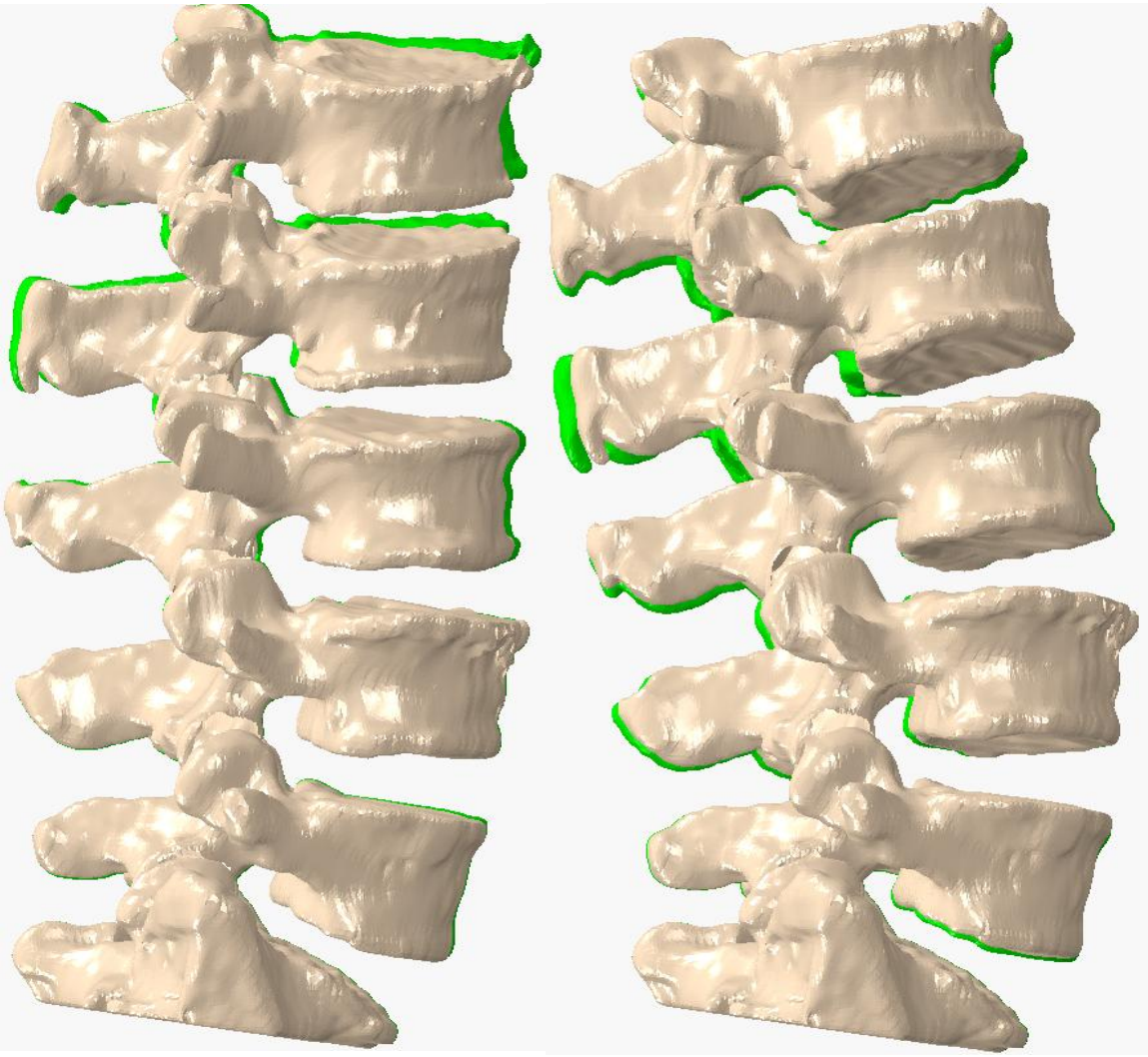

Figure 4.10 Overlay comparison of marker-displacement controlled model (green) and force controlled model in flexion + right lateral bend (left) and extension + left lateral bend (right).

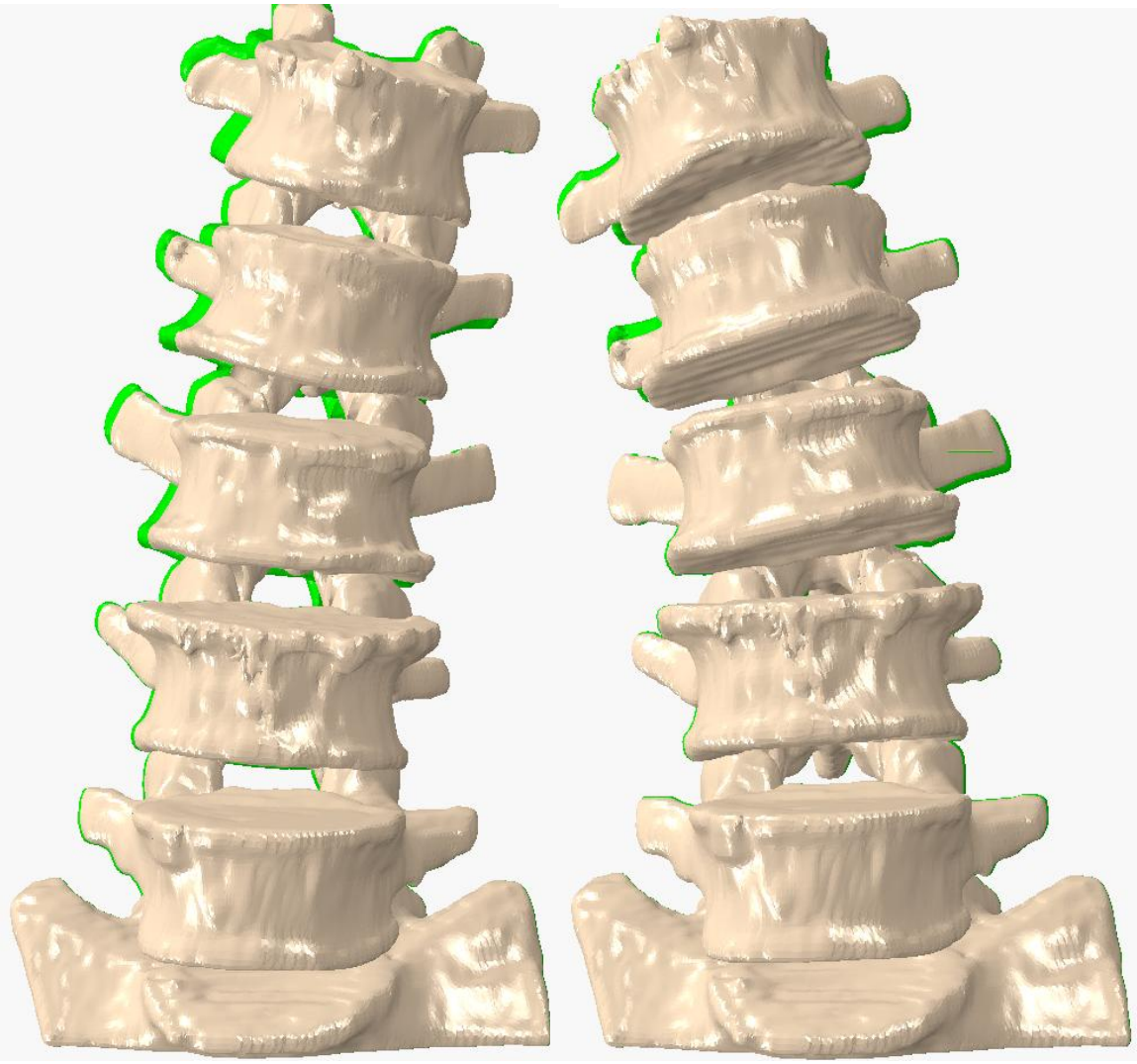

Figure 4.11 Overlay comparison of marker-displacement controlled model (green) and force controlled model in flexion + left lateral bend (left) and extension + right lateral bend (right).

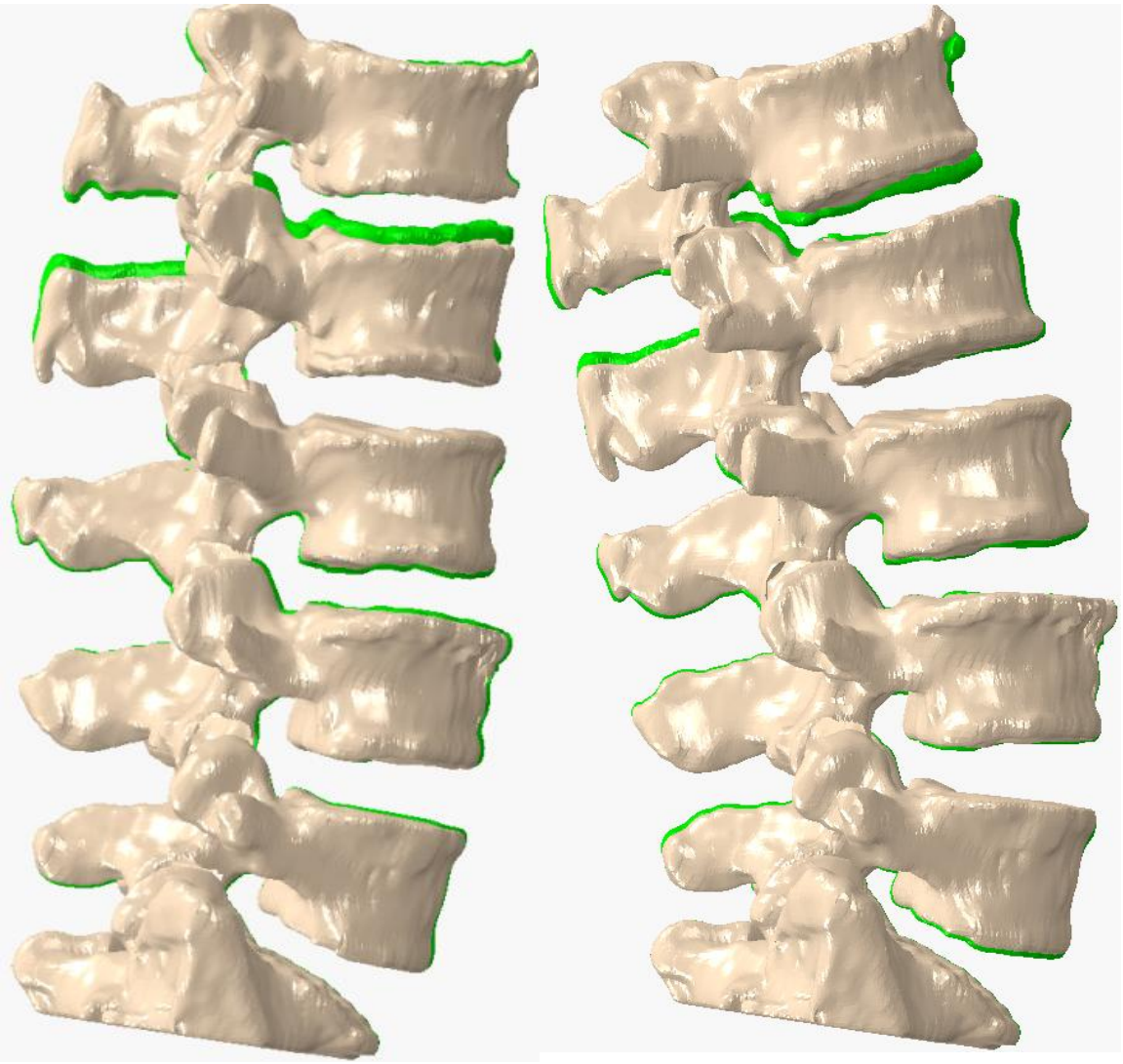

Figure 4.12 Overlay comparison of marker-displacement controlled model (green) and force controlled model in flexion + counterclockwise axial rotation (left) and extension + clockwise axial rotation (right).

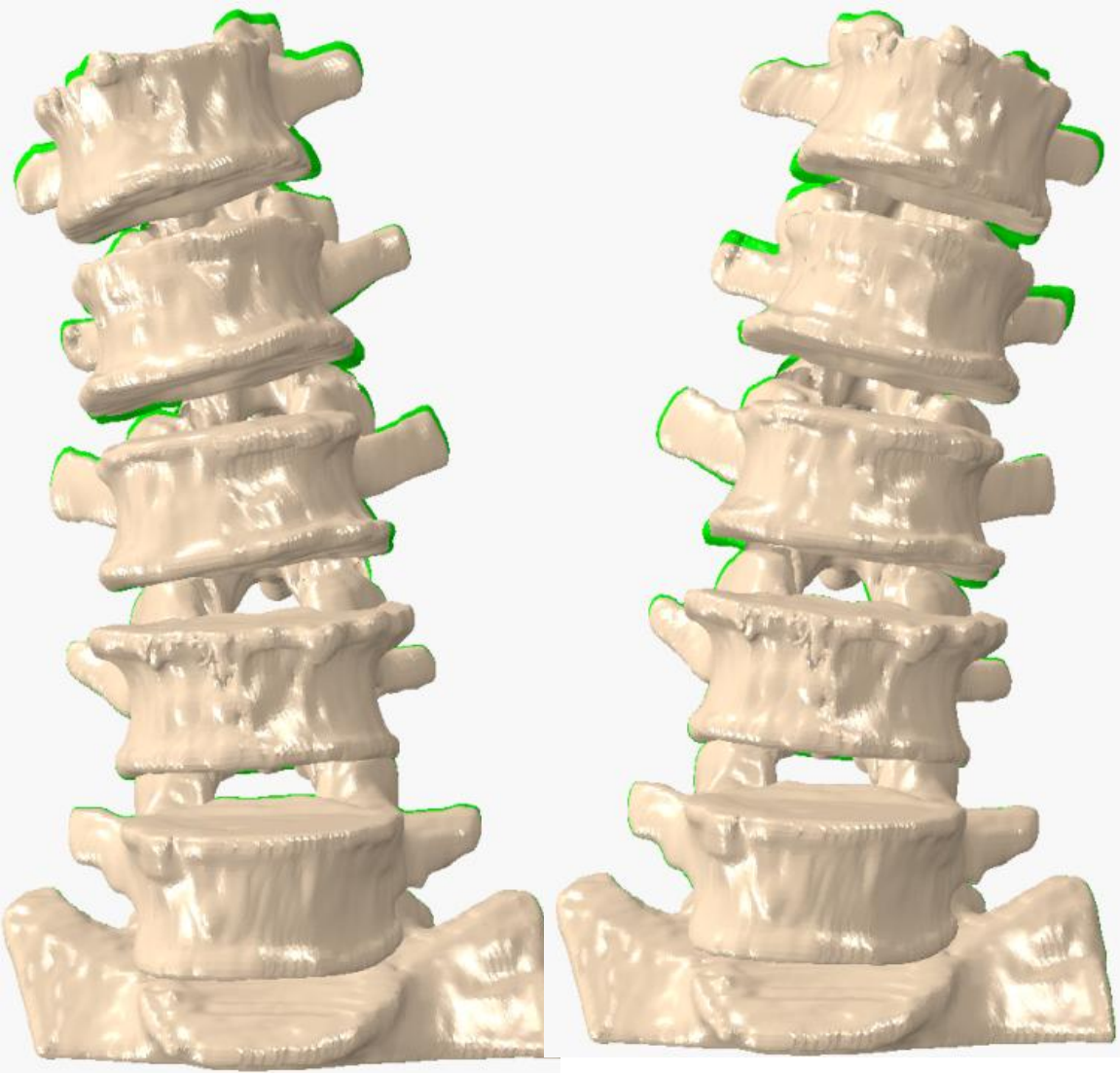

Figure 4.13 Overlay comparison of marker-displacement controlled model (green) and force controlled model in right lateral bend + clockwise axial rotation (left) and left lateral bend + counterclockwise axial rotation (right).

CHAPTER 5 – PREDICTION OF SPINE KINEMATICS FOLLOWING POSTERIOR STABILIZATION DEVICE INCLUSION

5.1 Introduction

One of the primary advantages of the finite element platform is the ability to define structures as rigid or deformable within the model, and to include a device. Previous chapters looked at the use of rigid bones without any deformable structures or implants for optimum computational efficiency. Although this is useful for timely prediction of spine kinematics and range of motion of the healthy, uninstrumented spine, the true usefulness of the finite element platform is the ability to predict information that cannot be obtained through experimental testing or rigid body modeling platforms such as strains in an implant or the annulus of the disc.

There are various combinations of rigid and deformable structures that can be included in the model. To evaluate changes in kinematics and range of motion as a result of device inclusion, and strains experienced by the device during motion, a device can simply be added to the rigid, computationally efficient model, providing a timely solution. Analysis time will increase as a result of including the deformable device; however, analysis times will continue to be significantly less than the fully deformable representation, while still providing a wealth of information about the device's performance. These kinds of analyses can be performed with both the FSU and multi-

segment models, depending on whether computational efficiency or adjacent level information is of higher priority.

The FE modeling platform is extremely versatile and can not only combine a deformable device with the computationally efficient FSU and multi-segment models, it can also be altered to hybrid rigid/deformable set up that combines a deformable level or levels with computationally efficient levels. This setup may involve a deformable level at L4-L5 and the computationally efficient bushing representation at all other levels. Depending on what structures are represented as deformable or rigid at the L4-L5 level, information such as strains in the annulus, bones, and device, as well as contact mechanics in the facets could potentially be calculated. There are several different representations that could be used that will vary in analysis time, ranging from the computationally efficient FSU, to the hybrid multi-segment model with a combination of rigid and deformable levels and device. Devices such as posterior pedicle stabilization implants are designed to limit range of motion and unload structures such as the disc and facets. The addition of a device to the computationally efficient FSU provides a timely method to predict changes in range in motion and the ability of the device to prevent painful positions.

5.2 Methods

5.2.1 Computationally Efficient and Fully Deformable Finite Element Models of the L4-L5 FSU with Titanium Rods

To demonstrate the usefulness of the computationally efficient L4-L5 FSU discussed prior for clinical and design phase assessment of device performance, a posterior stabilization device was added to the computationally efficient FSU model, as well as the fully deformable model. Four screws were implanted through the pedicles of L4 and L5 and two cylindrical rods vertically joined each pair of pedicle screws. Because the bones in this case remained rigid, node sets of each screw were beamed to the rigid body reference node of the vertebrae they were implanted in to simulate the connection between the bone and the screw. The rods were beamed to the posterior ends of the screws. The screws were represented as rigid bodies. Titanium rods were used for this analysis to compare the range of motion predicted by the computationally efficient and fully deformable models. The properties used for the titanium rods were a 110 GPa elastic modulus and 0.342 poison's ratio. Overall, the computationally efficient model consisted of rigid bones, a bushing connector element between L4 and L5 to represent the kinematic constraints that would be provided by the soft tissue structures and facets, rigid screws, and deformable rods. The fully deformable model consisted of rigid bones, deformable ligaments and disc, rigid screws, and deformable rods.

5.2.2 Computational Kinematic Analysis

Posterior stabilization devices are designed to limit the range of motion of the degenerated segment to avoid extreme motions which cause abnormal loading of anatomical structures. In earlier analysis the stiffness properties of the degree of freedom connector element were optimized to accurately reproduce the torque-rotation behavior of the cadaveric specimen when loaded with a pure moment using a spine simulator. This tuned model was then used to predict the changes in range of motion of the FSU following implantation of a posterior stabilization device with titanium rods. Results were compared to the fully deformable model. The models were run in flexion and extension and pure moments of ±10 Nm were applied to L4 while L5 was fully fixed, to be consistent with the experimental procedure. The rotation at the L4 rigid body reference node was requested as on output of the simulation and the torque-rotation behavior was plotted, comparing the uninstrumented and titanium implant cases.

5.3 Results

The ROM prediction of the computationally efficient model agreed well with the fully deformable representation for both the uninstrumented and implanted cases. The uninstrumented computationally efficient FSU with all soft tissue structures intact rotated 3.43 degrees in flexion and 3.40 degrees in extension with the application of ± 10 Nm at L4. Addition of the titanium posterior stabilization device significantly reduced the

FSU's range of motion. With titanium rods the FSU experienced maximum rotations of 0.2 degrees and 0.25 degrees in flexion and extension, respectively.

5.4 Discussion

In the past, evaluation of a device's performance has been a long and potentially expensive process. Cadaver testing requires the ability to obtain specimens, a facility where testing can be performed on human tissue, and test equipment to apply loading such as a spine simulator. Often times this kind of work is outsourced to a research group that specializes in this type of testing, which can be very expensive. Computational models alleviate the need for specialized testing facilities and equipment. Rigid body modeling platforms are limited by their lack of ability to predict internal stresses and strains. Finite element analysis is being utilized more often in the study of orthopaedic biomechanics. FE models save time and money relative to experimental testing. They are able to predict kinematic information, but also improve upon experimental testing and rigid body models because of their ability to predict internal stresses and strains.

The models described in this thesis improve upon existing FE models of the spine because of the computational efficiency. While simulations with deformable models may take several hours, the computationally efficient model can run an analysis in 1 minute. The ease of which a device can be added to the existing FE model and the subsequent ability of the model to predict changes in range of motion was demonstrated here. For these analyses bones and screws were modeled as rigid for optimum computational efficiency. Posterior stabilization devices are designed to limit range of motion and avoid

potentially painful positions. Titanium is a very stiff material commonly used for the rods in these applications. As expected, addition of the device to the model significantly reduced the range of motion of the FSU in flexion and extension. A comparison was made to the fully deformable model to confirm the accuracy of the prediction. While experimental testing is capable of providing the same information, it would be significantly more expensive and time consuming. It is possible to add the device to the model, run the analysis, and have results within a few hours.

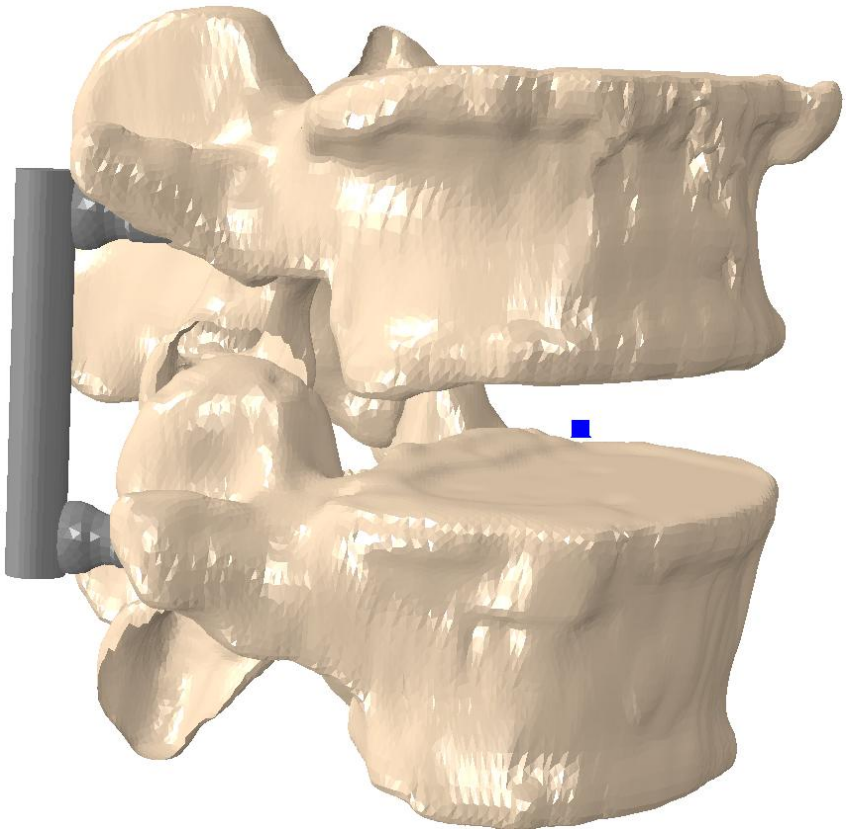

Figure 5.1 L4-L5 FSU instrumented with posterior stabilization device. Screws inserted through the pedicles. Rods modeled as titanium.

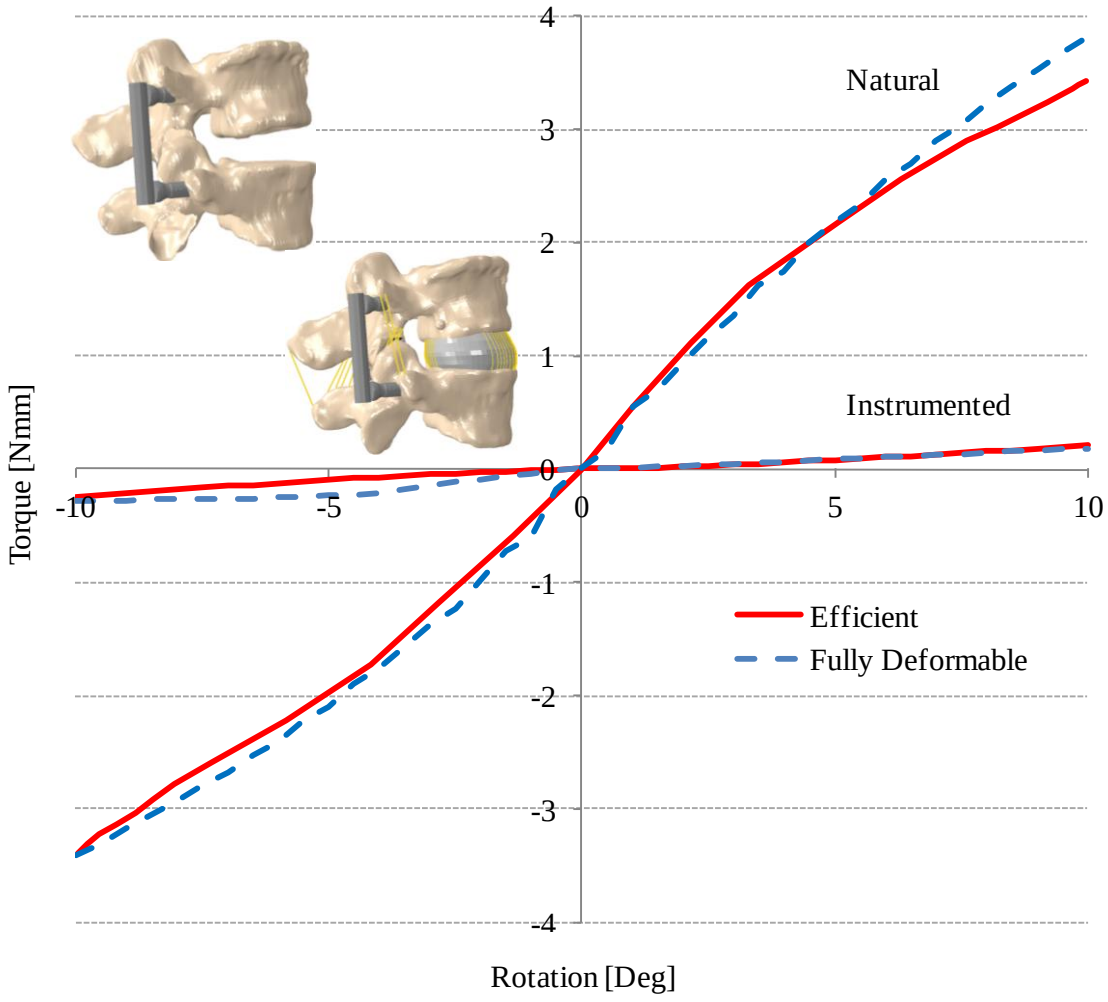

Figure 5.2 Comparison of torque-rotation behavior for intact FSU and FSUs instrumented with titanium and PEEK posterior fusion rods.

CHAPTER 6 - DISCUSSION AND CONLCUSIONS

The study of orthopaedic biomechanics has evolved from experimental techniques dominating the field, to the emergence and frequent use of computational simulations. Although there are many advantages of computational models, they will never fully replace experimental studies. The data that is collected through experiments make it possible to develop and validate computational models. The use of rigid body and FE modeling platforms to study and predict biomechanics is rapidly growing. Many spine models have been developed within rigid body modeling platforms which can effectively predict kinematics of the vertebral bodies. These platforms have also been used to develop complex musculoskeletal models. The obvious difference between rigid body and FE platforms is the ability of the FE platforms to predict internal stresses and strains of structures in the model. The use of FEA to study biomechanics is becoming increasingly popular due to the ability to predict information that cannot obtained in experimental cadaver studies and with rigid body models.

The primary drawback of current FE spine models is the long analysis times. The inclusions of deformable structures such as the disc and ligaments which experience large deformations make the largest contributions to long analysis times. If strains in these structures are not of interest then inclusion of these structures unnecessarily drive up analysis times. Reduced run times would make FE models more useful for evaluating new devices and for optimizing muscle parameters in musculoskeletal models, which

require the ability to quickly run multiple analyses. In this study a computationally efficient L4-L5 FSU and a L1-S1 multi-segment model were developed and tuned. Model validation was possible due to available kinematic data collected during prior experimental testing on the spine segments. The goal was to develop models that could accurately predict spine mechanics with a shorter analysis times than current deformable models. Previous efforts to accomplish this have been made. A ball and socket mechanical constraint was used between vertebrae to provide rotational stiffness to the model. This approach was successful in reducing analysis time and producing the proper torque-rotation response, however, translational degrees of freedom were neglected. This modeling approach was based on the assumption that movement of vertebral bodies was purely rotational. Although translation of vertebral bodies is relatively small, they are nonzero and should be accounted for to accurately represent spine motion. This was accomplished through the use of a bushing connector element between adjacent vertebrae to provide rotational and translational stiffness to the model. Overlays of the force controlled model and marker-displacement controlled model confirmed that the model was producing the appropriate torque-rotation response, as well as the overall motion of the spine. This was accomplished while also reducing the analysis times for the FSU and multi-segment model from hours to a few minutes.

The FSU consists of the L4 and L5 vertebrae. This model has the shortest analysis time and is ideally suited for running multiple analyses in a short amount of time. The stiffness of the bushing was tuned to represent the FSU with varying levels of intact soft tissue structures. This makes the model useful for studying the contributions of individual structures to the overall mechanical stability of the segment. As demonstrated in chapter

5, this model can be used as a tool to evaluate the performance of an implant. In this study a posterior stabilization device was added to the model. These devices are used to limit the range of motion of the segment and avoid potentially painful positions. The model was used to predict changes in range of motion following instrumentation with titanium rods, and demonstrated that it can make the prediction effectively. To make further assessments of the device, the model could be used to predict strains in the device and bones, or stresses in the facets. The primary limitation of this model is that it is specific to one level, and cannot provide information about adjacent segment mechanics. Fusion procedures often lead to degeneration at adjacent levels, which makes mechanics at adjacent levels a point of interest. Overall, this model provides an efficient method to evaluate device performance and study spine mechanics at the L4-L5 level.

The multi-segment model consists of L1 through the sacrum. Stiffness of the bushings were tuned to represent the spine segment with all soft tissue structures intact. Although having multiple levels causes the analysis time for the model to be slightly longer than the FSU, it is still significantly faster than the deformable model. As stated above, adjacent segment mechanics are important when evaluating the effects of an implant on the spine. This is the main advantage that the multi-segment model has over the FSU. The multi-segment will also serve as a useful tool for future efforts to develop a lumbar musculoskeletal model. Optimization of muscle parameters requires multiple analyses, making the computationally efficient model ideal for this application.

Ultimately this study was a success. These computationally efficient models are able to accurately predict the mechanics of the spine segment with significantly reduced analysis times, relative to the fully deformable model. One area where the model could be

improved is the tuning of the stiffness of the translational degrees of freedom. Force and translational data was collected during pure moment loading, which was used for tuning these degrees of freedom. However, no testing was specifically performed with the intention of understanding the response of the segments in response to shear loads. The available data was sufficient to tune the stiffness of translational degrees of freedom in response to a torque, but future cadaver testing should include shear testing to gain a better understanding of the stiffness of the segment in response to shear loads.

List of References

Cerciello, T., Romano, M., Bifulco, P., Cesarelli, M. Allen, R., "Advanced template matching method for estimation of intervertebral kinematics of lumbar spine," *Medical Engineering and Physics,* doi:10/1016/j.megengphy.2011.06.09 (2011).

Duquesnoy, B., Allert, F.A., Verdoncq, B., "Psychosocial and occupational impact of chronic low back pain," *Rev Rhum Engl Ed*., Vol. 65, pp. 33-40 (1998).

van Tulder, M.W., Koes, B., Malmivaara, A., "Outcome of non-invasive treatment modalities on back pain: an evidence based review. *European Spine Journal,* Vol. 15, pp. 564-581 (2006).

Krismer, M., van Tulder, M., "Low back pain (non-specific)," *Best Practice & and Research Clinical Rheumatology,* Vol. 21, pp. 77-91 (2007).

Manek, N.J., MacGregor, A.J., "Epidemiology of back disorders: prevelance, risk factors, and prognosis," *Current Opinion in Rheumatology,* Vol. 17, pp. 134-40 (2005).

Katz, J.N., "Lumbar Disc Disorders and Low-Back Pain: Socioeconomic Factors and Consequences," *Journal of Bone and Joint Surgery (American),* Vol. 88, pp. 21-24 (2006).

Panjabi, M.M., "Clinical spinal instability and low back pain," *Journal of Electromyography and Kinesiology,* Vol. 13, pp. 371-9 (2003).

Panjabi, M.M., "The stabilizing system of the spine, Part II. Neutral zone and instability hypothesis," *Journal of Spinal Disorders & Techniques,* Vol. 4, pp. 390-6 (1992).

Fujiwara, A., Lim, T.H., An, H.S., Tanaka, N., Jeon, C.H., Anderson, G.B., Haughton, V.M., "The effect of disc degeneration and facet joint osteoarthritis on the segmental flexibility of the lumbar spine," *Spine,* Vol. 25, pp. 3036-44 (2000).

Gertzbein, S.D., Seligman, J., Holtby, R., Chan, K.H., Kapasouri, A., Tile, M., Cruickshank, B., "Centrode patterns and segmental instability in degenerative disc disease," *Spine,* Vol. 10, pp. 257-261 (1985).

Dickey, J,P., Pierrynowski, M.R., Bednar, D.A., Yang, S.X., "Relationship between pain and vertebral motion in chronic low-back pain subjects," *Clinical Biomechanics,* Vol. 17, pp. 345-52 (2002).

Vernon-Roberts, B., Pirie, C.J., "Degenerative changes in the intervertebral discs of the lumbar spine and their sequelae," *Rheumatology,* Vol. 16, pp. 13-21 (1977).

Noailly, J., Ambrosio, L., Tanner, K.E., Planell, J.A., Lacroix, D., 'In silico evaluation of a new composite disc substitute with a L3-L5 lumbar spine finite element model," *European Spine Journal,* DOI 10.1007/s00586-011-1716-7, online first (2011).

Wilke, H.J., Rohlmann, F., Neidlinger-Wilke, C., Werner, K., Claes, L., Kettler, A., "Validity and interobserver agreement of a new radiographic grading system for intervertebral disc degeneration: part I. Lumbar Spine," *European Spine Journal,* Vol. 15, pp. 720-730 (2006).

Haefeli, M., Kalberer, F., Saegesser, D., Nerlich, A.G., Boos, N., Paesold, G., "The course of macroscopic degeneration in the human lumbar intervertebral disc," *Spine Journal,* Vol. 31, pp. 1522-1531 (2006).

Adams, M.A., Dolan, P., "Spine Biomechanics," *Journal of Biomechanics,* Vol. 38, pp. 1972-1983 (2005).

Mulholland, R.C., "The myth of lumbar instability: the importance of abnormal loading as a cause of low back pain," *European Spine Journal,* Vol. 17, pp. 619-625 (2008).

Nakamura, T., Iribe, T., Asou, Y., Miyairi, H., Ikegami, K., Takakuda, K., "Effects of compressive loading on biomechanical properties of disc and peripheral tissue in a rat tail model," *European Spine Journal,* Vol. 18, pp. 1595-1603, (2009).

Setton, L.A., Chen, J., "Mechanobiology of the intervertebral disc and relevance of disc degeneration," *Journal of Bone and Joint Surgery (American),* Vol. 88, pp. 52-57, (2006).

Viderman, T., Markku, N.M., "The Occurance of Annular Tears and Their Relation to Lifetime Back Pain History: A cadaveric Study Using Barium Sulfate Discography," *Spine Journal,* Vol. 29, pp. 2668-76, (2004).

Mixter, W.J., Barr, J.S., "Rupture of the intervertebral disc with involvement of the spinal canal," *New England Journal of Medicine,* Vol. 211, pp. 210-215, (1934).

Ekman, M., Jonhagen, S., Hunsche, E., Jonsson, L., "Burden of Illness of Chronic Low Back Pain in Sweden. A cross-sectional, Retrospective Study in Primary Care Setting," *Spine Journal,* Vol. 30, pp. 1777-85, (2005).

Waddell, G., Burton, A.K., "Concepts of Rehabilitation for the Management of Low Back Pain," *Best Practice and Research Clinical Rheumatology,* Vol. 19, pp. 655-70, (2005).

Jim, J.T.J., Noponen-Hietala, N., Cheung, K.M.C., Ott, J., Karppinen, J., et al., "The TRP2 Allele of COL9A2 is an Age-Dependent Risk Factor for the Development and Severity of Intervertebral Disc Degeneration," *Spine Journal,* Vol. 30, pp. 2735–42, (2005).

Galbusera, F., Bellini, C.M., Anasetti, F., Ciavarro, C., Lovi, A., Brayda-Bruno, M., "Rigid and flexible spinal stabilization devices: A biomechanical comparison," *Medical Engineering and Physics*, Vol. 33, pp. 490-6, (2011).

Sengupta, D.K., "Dynamic stabilization devices in the treatment of low back pain," *Orthopedic Clinics of North America*, Vol. 35, pp. 43-56, (2004).

Freeman, B.J.C., Davenport, J., "Total disc replacement in the lumbar spine: a systematic review of the literature," *European Spine Journal*, Vol. 15, pp. 439-47, (2006).

Don, A.S., Carragee, E., "A brief overview of evidence-informed management of chronic low back pain with surgery," *Spine Journal*, Vol. 8, 259-65, (2008).

Ekman, P., Moller, H., Tullberg, T., Neumann, P., Hedlund, R., "Posterior Lumbar Interbody Fusion Versus Posterolateral Fusion in Adult Isthmic Spondylolisthesis," *Spine Journal*, Vol. 32, pp. 2178-83, (2007).

Fritzell, P., Hagg, O., Nordwall, A., "Complications in lumbar fusion surgery for chronic low back pain: a comparison of three surgical techniques used in a prospective randomized study. A report from the Swedish lumbar spine," *European Spine Journal*, Vol. 12, pp. 178-189, (2003).

Guyer, R.D., McAfee, P.C., Banco, R.J., Bitan, F.D., Cappuccino, A., Geisler, F.H., Hochschuler, S.H., Holt, R.T., Jenis, L.G., Majd, M.E., Regan, J.J., Tromanhauser, S.G., Wong, D.C., Blumenthal, S.L., "Prospective randomized multicenter Food and Drug Administration investigational device exemption study of lumbar total disc replacement with the CHARITE artificial disc versus lumbar fusion: five-year follow-up," *Spine Journal*, Vol. 9, pp. 374-86, (2009).

Zigler, J., Delamarter, R., Spivak, J.M., Linovitz, R.J., Danielson III, G.O., Haider, T.T., Cammisa, F., Zuchermann, J., Balderston, R., Kitchel, S., Foley, K., Watkins, R., Bradford, D., Yue, J., Yuan, H., Herkowitz, H., Geiger, D., Bendo, J., Peppers, T., Sachs, B., Girardi, F., Kropf, M., Goldstein, J., "Results of the prospective randomized multicenter Food and Drug Administration investigational device exemption study of the ProDisc-L total disc replacement versus circumferential fusion for the treatment of 1-level degenerative disc disease," *Spine Journal*, Vol. 32, pp. 1155-62, (2007).

Berg, S., "On total disc replacement," *Acta Orthopaedica* by Informs Healthcare, (2011).

Gray, H., "Gray's Anatomy A Facsimile," TAJ Books, Cobham, Surray, United Kingdom, (2001).

Blumethal, S., McAfee, Paul, C., Guyer, R., Hochschuler, S., Geisler, F., Holt, R,T., Garcia Jr, R., Regan, J.J., Ohnmeiss, D,D., "A Prospective, Randomized, Multicenter Food and Drug Administration Investigational Device Exemptions Study of Lumbar Total Disc Replacement With the CHARITE Artificial Disc Versus Lumbar Fusion: Part I: Evaluation of Clinical Outcomes," *Spine Journal,* Vol. 30, pp. 1565-75, (2005).

Dmitriev, A.E., Gill, N.W., Kuklo, T.R., Rosner, M.K., "Effect of multilevel lumbar disc arthroplasty on the operative- and adjacent-level kinematics and intradiscal pressures: an in vitro human cadaveric assessment," *Spine Journal,* Vol. 8, pp. 918-25, (2008).

Kanayama, M., Togawa, D., Hashimoto, T., Shigenobu, K., Oha, F., "Motion-preserving Surgery Can Prevent Early Breakdown of Adjacent Segments: Comparison of Posterior Dynamic Stabilization With Spinal Fusion," *Journal of Spinal Disorders & Techniques,* Vol. 22, pp. 463-7, (2009).

Anderson, P.A., Rouleau, J.P., "Intervertebral Disc Arthroplasty," *Spine Journal,* Vol. 29, pp. 2779-2786, (2004).

Lemaire, J.P., Carrier, H., El-Hadi, S., Skalli, W., Lavaste, F., "Clinical and Radiological Outcomes With the Charite Artificial Disc: a 10- Year Minimum Follow-Up,"*Journal of Spinal Disorders & Techniques,* Vol.18, pp. 353-9, (2005).

Tropiano, P., Huang, R.C., Girardi, F.P., Cammisa, F.P., Marnay, T., "Lumbar total disc replacement. Seven to eleven-year follow-up," *Journal of Bone and Joint Surgery (American),* Vol. 87, pp. 490-6, (2005).

Bertagnoli, R., Kumar, S., "Indications for full prosthetic disc arthroplasty: a correlation of clinical outcome against a variety of indications," *European Spine Journal,* Vol. 11, pp. 131-6, (2002).

Bertagnoli, R., Yue, J.J., Shah, R.V., Nanieva, R., Pfeiffer, F., Fenk-Mayer, A., Kershaw, T., Husted, D.S., "The Treatment of Disabling Multilevel Lumbar Discogenic Low Back Pain With Total Disc Arthroplasty Utilizing the ProDisc Prosthesis: A Prospective Study With 2-Year Minimum Follow-up," *Spine Journal,* Vol. 30, pp. 2192-99, (2005).

Chung, S.S., Lee, C.S., Kang, C.S., "Lumbar Total Disc Replacement Using ProDisc II: A Prospective Study With a 2-Year Minimum Follow-up," *Journal of Spinal Disorders & Techniques,* Vol. 19, pp. 411-5, (2006).

Le Huec, J.C., Mathews, H., Basso, Y., Aunoble, S., Hoste, D., Bley, B., Friesem, T., "Clinical Results of Maverick Lumbar Total Disc Replacement: Two-Year Prospective Follow-up," *Orthopedic Clinics of North America,* Vol. 36, pp. 315-22, (2005).

Lemaire, J.P., Skalli, W., Lavaste, F., Templier, A., Mendes, F., Diop, A., Sauty, V., Laloux, E., "Intervertebral Disc Prosthesis: Results and Prospects for the Year 2000," *Clinical Orthopaedics & Related Research,* Vol. 337, pp. 64-76, (1997).

Shim, C.S., Lee, S., Shin, H., Kang, H.S., Choi, W., Jung, B., Choi, G., Ahn, Y., Lee, S., Lee, H.Y., "CHARITE Versus ProDisc: A Comparative Study of A Minimum 3-Year Follow-up," *Spine Journal,* Vol. 32, pp. 1012-8, (2007).

Siepe, C.J., Mayer, H.M., Wiechert, K., Korge, A., "Clinical Results of Total Lumbar Disc Replacement With ProDisc II: Three-Year Results for Different Indications," *Spine Journal,* Vol. 31, pp. 1923-32, (2006).

Tropiano, P., Huang, R.C., Girardi, F.P., Marnay, T., "Lumbar Disc Replacement: Preliminary Results with ProDisc II After a Minimum Follow-Up Period of 1 Year," *Journal of Spinal Disorders & Techniques,* Vol. 16, pp. 362-8, (2003).

Zeegers, W.S., Bohnen, L.M.L.J., Laaper, M., Verhaegen, M.J.A., "Artificial disc replacement with the modular type SB Charite III: 2-year results in 50 prospectively studied patients," *European Spine Journal,* Vol. 8, pp. 210-7, (1999).

Sinigaglia, R., Bundy, A., Costantini, S., Nena, U., Finocchiaro, F., Monterumici, D.A., "Comparison of single-level L4-L5 versus L5-S1 lumbar disc replacement: results and prognostic factors," *European Spine Journal,* Vol. 18, pp. 52-63, (2009).

Putzier, M., Funk, J.F., Schneider, S.V., Gross, C., Tohtz, S.W., Khodadayan-Klostermann, C., Perka, C., Kandziora, F., "Charite total disc replacement—clinical and raiographical results after an average follow-up of 17 years," *European Spine Journal,* Vol. 15, pp. 183-95, (2006).

Siepe, C.J., Korge, A., Grochulla, F., Mehren, C., Mayer, M., "Analysis of post-operative pain patterns following total lumbar disc replacement: results from fluoroscopically guided spine infiltrations," *European Spine Journal,* Vol. 17, pp. 44-56, (2008).

Mulholland, R.C., "The myth of lumbar instability: the importance of abnormal loading as a cause of low back pain," *European Spine Journal,* Vol. 17, pp. 619-25, (2008).

Andersson, G.B.J., An, H.S., Oegema, T.R., Setton, L.A., "Directions for future research," *Journal of Bone and Joint Surgery (American),* Vol. 88A, pp. 110-14, (2006).

Harman, P.H., "Indications for Spinal Fusion in Lumbar Diskopathy, Instability and Arthrosis," *Clinical Orthopaedics & Related Research,* Vol. 34, pp. 73-91, (1964).

Yan, J.Z., Qiu, G.X., Wu, Z.H., Wang, X.S., Xing, Z.J., "Finite element analysis in adjacent segment degeneration after lumbar fusion," *The International Journal of Medical Robotics And Computer Assisted Surgery,* Vol. 7, pp. 96-100, (2011).

Fritzell, P., Hagg, O., Wessberg, P., Nordwall, A., "2001 Volvo Award Winner in Clinical Studies: Lumbar Fusion Versus Nonsurgical Treatment for Chronic Low Back Pain: A Multicenter Randomized Controlled Trial From the Swedish Lumbar Spine Study Group," *Spine Journal,* Vol. 26, pp. 2521-32, (2001).

Wilke, H.J., Heuer, F., Schmidt, H., "Prospective Design Delineation and Subsequent In Vitro Evaluation of a New Posterior Dynamic Stabilization System," *Spine Journal,* Vol. 34, pp. 255-61, (2009).

Min, J.H., Jang, J.S., Jung, B.J., Lee, H.Y., Choi, W.C., Shim, C.S., Choi, G., Lee, S.H., "The Clinical Characteristics and Risk Factors for the Adjacent Segment Degeneration in Instrumented Lumbar Fusion," *Journal of Spinal Disorders & Techniques*, Vol. 21, pp.305-9, (2008).

Aota, Y., Kumano, K., Hirabayashi, S., "Postfusion instability at the adjacent segments after rigid pedicle screw fixation for degenerative lumbar spinal disorders," *Journal of Spinal Disorders,* Vol. 8, pp. 464-73, (1995).

Anderst, W.J., Vaidya, R., Tashman, S., "A technique to measure three-dimensional in vivo rotation of fused and adjacent lumbar vertebrae," *Spine Journal,* Vol. 8, pp. 991-7, (2008).

Rohlman, A., Zander, T., Rao, M, Bergmann, G., "Applying a follower load delivers realistic results for simulating standing," *Journal of Biomechanics,* Vol. 42, pp. 1520-6, (2009a).

Rohlman, A., Zander, T., Rao, M., Bergmann, G., "Realistic loading conditions for upper body bending," *Journal of Biomechanics,* Vol. 42, pp. 884-90, (2009b).

Christophy, M., Senan, N.A.F., Lotz, J.C., O'Reilly, O.M., "A Musculoskeletal model for the lumbar spine," *Biomechanics and Modeling in Mechanobiology,* DOI 10.1007/s10237-011-0290-6

de Zee, M., Hansen, L., Wong, C., Rasmussen, J., Simonsen, E.B., "A generic detailed rigid-body lumbar spine model," *Journal of Biomechanics,* Vol. 40, pp. 1219-27, (2006).

El-Rich, M., Shirazi-Adl, A., Arjmand, N., "Muscle Activity, Internal Loads, and Stability of the Human Spine in Standing Postures: Combined Model and In Vivo Studies," *Spine Journal,* Vol. 29, pp. 2633-42, (2004).

Huynh, K.T., Gibson, I., Lu, W.F., Jagdish, B.N., "Simulating Dynamics of Thoracolumbar Spine Derived from LifeMOD under Haptic Forces," *World Academy of Science, Engineering and Technology,* Vol 64, pp. 278-85, (2010).

Liu, Y.S., Tsay, T.S., Wang, T.C., "Muscles force and joints load simulation of bicycle riding using multibody models," *Procedia Engineering,* Vol. 13, pp. 81-7, (2011).

Lambrecht, J.M., Audu, M.L., Triolo, R.J., Kirsch, R.F., "Musculoskeletal model of trunk and hips for development of seated-posture-control neuroprosthesis," *Journal of Rehabilitation Research & Development,* Vol. 46, pp. 515-28, (2009).

Natarajan, R.N., Williams, J.R., Andersson, G.B.J., "Modeling changes in intervertebral disc mechanics with degeneration," *Journal of Bone and Joint Surgery (American),* Vol. 88A, pp. 36-40, (2005).

Rohlmann, A., Zander, T., Schmidt, H., Wilke, H.J., Bergmann, G., "Analysis of the influence of disc degeneration on the mechanical behaviour of a lumbar motion segment using the finite element method," *Journal of Biomechanics,* Vol. 39, pp. 2484-90, (2006).

Schmidt, H., Shirazi-Adl, A., Galbusera, F., Wilke, H.J., "Response analysis of the lumbar spine during regular activities-A finite element analysis," *Journal of Biomechanics,* Vol. 43, pp. 1849-56, (2010).

Shirazi-Adl, S.A., Shrivastava, S.C., Ahmed, A., "Stress Analysis of the Lumbar Disc-Body Unit in Compression A Three-Dimensional Nonlinear Finite Element Study," *Spine Journal,* Vol. 9, pp. 120-34, (1984).

Lu, M.Y., Hutton, W., Gharpuray, V., "Can Variations in Intervertebral Disc Height Affect the Mechanical Function of the Disc?" *Spine Journal,* Vol. 21, pp. 2208-16, (1996).

Zander, T., Rohlmann, A., Calisse, J., Bergmann, G., "Estimation of muscle forces in the lumbar spine during upper-body inclination," *Clinical Biomechanics,* Vol. 16, pp. 73-80, (2001).

Schmidt, H., Heuer, F., Simon, U., Kettler, A., Rohlmann, A., Claes, L., Wilke, H.J., "Application of a new calibration method for a three-dimensional finite element model of a human lumbar annulus fibrosus," *Clinical Biomechanics,* Vol. 21, pp. 337-44, (2006).

Jones, A.C., Wilcox, R.K., "Finite element analysis of the spine: Towards a framework of verification, validation and sensitivity analysis," *Journal of Medical Engineering & Physics,* Vol. 30, pp. 1287-304, (2008).

Goel, V.K., Monroe, B.T., Gilbertson, L.G., Brinckmann, P., "Interlaminar Shear Stresses and Laminae Seperation in a Disc: Finite Element Analysis of the L3-L4 Motion Segment Subjected to Axial Compressive Loads," *Spine Journal,* Vol. 20, pp. 689-98, (1995).

Liebschner, M.A.K., Kopperdahl, D.L., Rosenberg, W.S., Keaveny, T.M., "Finite Element Modeling of the Human Thoracolumbar Spine," *Spine Journal,* Vol. 28, pp. 559-65, (2003).

Adams, M.A., McNally, D.S., Dolan, P., "'STRESS' DISTRIBUTIONS INSIDE INTERVERTEBRAL DISCS," *Journal of Bone & Joint Surgery,* Vol. 78, pp. 965-72, (1996).

Frei, H., Oxland, T.R., Rathonyi, G.C., Nolte, L.P., "The Effect of Nucleotomy on Lumbar Spine Mechanics in Compression and Shear Loading," *Spine Journal,* Vol. 26, pp. 2080-9, (2001).

Heuer, F., Schmidt, H., Claes, L., Wilke, H.J., "Stepwise reduction of functional spinal structures increase vertebral translation and intradiscal pressure," *Journal of Biomechanics,* Vol. 40, pp. 795-803, (2007).

Sawa, A.G.U., Crawford, N.R., "The use of surface strain data and a neural networks solution method to determine lumbar facet joint loads during in vitro spine testing," *Journal of Biomechanics,* Vol. 41, pp. 2647-53, (2008).

Wilson, D.C., Niosi, C.A., Zhu, Q.A., Oxland, T.R., Wilson, D.R., "Accuracy and repeatability of a new method for measuring facet loads in the lumbar spine," *Journal of Biomechanics,* Vol. 39, pp. 348-53, (2006).

Godest, A.C., Beaugonin, M., Haug, E., Taylor, M., Gregson, P.J., "Simulation of a knee joint replacement during a gait cycle using explicit finite element analysis," *Journal of Biomechanics,* Vol. 35, pp. 267-75, (2001).

Abaqus 6.10 Documentation, Dassault Systemes Simulia Corp., Providence, RI, USA, (2010).

Chapra, S.C., "Numerical Methods for Engineers," *McGraw-Hill,* 6th Edition, New York, New York, (2010).

Venkataraman, P., "Applied Optimization with Matlab Programming," *John Wiley & Sons, Inc.,* Hoboken, New Jersey, (2009).

Isight 4.5 Documentation, Dassault Systemes Simulia Corp., Providence, RI, USA, (2010).

Murtagh, R.D., Quencer, R.M, Castellui, A.E., Yue, J.J., "New Techniques in Lumbar Spinal Instrumentation: What the Radiologist Needs to Know," *Radiology,* Vol. 260, pp. 317-30, (2011).